Maryland Water Resources Research Center
Annual Technical Report
FY 2017

Introduction

During Funding Year 2017, the Maryland Water Resources Research Center supported a range of water quality-related topics, including novel methods to assess the erosive power of streams and rivers, potential enhancement of microbial activity in wetland restoration, a new management approach to reduce nutrient runoff from drained farm fields, and understanding the transport and effects of road salt in surface and groundwater. The Center continues seeking to serve the diversity of Maryland geography, educational institutions, and students.

Research Program Introduction

Under the 2017 104(B) program, the Maryland Water Resources Research Center supported two faculty-led projects:

- 2017MD340B: Can Carbon Amendments Improve Wetland Restoration and Jump-Start Microbial Activity?
- 2017MD341B: Listening to Rivers: Seismic and Hydraulic Monitoring to Determine River Turbulence and Erosive Power

The 104(B) funds also supported three summer graduate student fellowships:

- 2017MD343B: Assessing nitrate reduction potential in Maryland's agricultural water resources
- 2017MD344B: Major ions, strontium isotopes, and geochemical cycling across a forested to urban gradient
- 2017MD345B: Seismo-Acoustic Observation of Cavitation and Erosive Potential in a Bedrock River

A supplemental project, in cooperation with the U.S. Army Corps of Engineers Institute for Water Resources, was also active during this period:

- 2016MD347S: Impact of the "308 Reports" on Water Resources Planning and Development in the United States and Implications of these Results for the Future.

Support for a FY2016 104(B) project concluded during FY2017:

- 2016MD336B: Assessing riparian hydrologic pathways as controls on forested buffer function in the Antietam Creek watershed, western Maryland

Finally, MWRRC continues to hold a 104(G) project originally awarded to a Maryland PI, while the PI is between academic appointments.

- 2014MD321G: Environmental Concentrations and Exposure Effects of Environmental Gestagens on a Sentinel Teleost Fish

Environmental Concentrations and Exposure Effects of Environmental Gestagens on a Sentinel Teleost Fish

Basic Information

Title:	Environmental Concentrations and Exposure Effects of Environmental Gestagens on a Sentinel Teleost Fish
Project Number:	2014MD321G
USGS Grant Number:	G14AS00014
Start Date:	9/1/2014
End Date:	8/31/2017
Funding Source:	104G
Congressional District:	MD-005
Research Category:	Water Quality
Focus Categories:	Water Quality, Toxic Substances, Wastewater
Descriptors:	None
Principal Investigators:	Edward F Orlando, Michael T Meyer, Patrick Phillips

Publications

There are no publications.

Status Report: 2014MD321G
Environmental Concentrations and Exposure Effects of Environmental Gestagens on a Sentinel Teleost Fish

Dr. Edward Orlando, PI, left his faculty position at the University of Maryland in July 2016. He continues to seek a new faculty position. As arranged with USGS, the Maryland Water Resources Research Center is holding this project, and will transfer it to Dr. Orlando when he has found his new position.

A no-cost extension was requested and granted per Modification No. 0001 to Award No. G14AP00169, dated 8/29/2017. The project's current end date is 8/31/2018.

An additional extension will be requested.

K. Brubaker, June 2018

Assessing riparian hydrologic pathways as controls on forested buffer function in the Antietam Creek watershed, western Maryland

Basic Information

Title:	Assessing riparian hydrologic pathways as controls on forested buffer function in the Antietam Creek watershed, western Maryland
Project Number:	2016MD336B
Start Date:	4/1/2016
End Date:	2/28/2018
Funding Source:	104B
Congressional District:	MD-006
Research Category:	Water Quality
Focus Categories:	Surface Water, Non Point Pollution, Nutrients
Descriptors:	None
Principal Investigators:	Keith N. Eshleman

Publications

There are no publications.

MWRRC Annual Report

Title:	Assessing riparian hydrologic pathways as controls on forested buffer function in the Antietam Creek watershed, western Maryland
Project Number:	G16AP00061 Z9212101 2016MD336B
Start Date:	March 1, 2016
End Date:	Feb. 28, 2018
Funding Source:	USGS State Water Resources Research Institute Program
Congressional District:	6
Research Category:	Water Quality
Focus Category:	Hydrogeology, Biogeochemistry, Water Quality, Conservation Practices
Descriptors:	None
Principal Investigators:	Keith Eshleman and Stephanie Siemek

Publications

There are no publications.

Completion Report

Assessing Riparian Buffers in the Ridge and Valley Province in Western Maryland

Prepared for: Maryland Water Resources Research Center

Project Number: G16AP00061 Z9212101
Project duration: March 1, 2016- Feb. 28, 2018
Principal Investigator: Keith Eshleman

Appalachian Laboratory
University of Maryland Center for Environmental Science
301 Braddock Road, Frostburg, MD 21532
keshleman@umces.edu
301-689-7170
Prepared by: K. Eshleman, S. Siemek (graduate student)
Submitted: *May 31, 2018*

I) Project Summary

A) Problem Statement

Excessive nutrients derived primarily from agricultural activities in the Chesapeake Bay watershed (CBW) have been found to cause noxious algal blooms in the Chesapeake Bay (Jordan et al., 1997; Malone et al. 1986, 1988; Boynton et. al. 1982; Jordan et al., 1991; Fisher et al. 1992; Gallegos et al. 1992). Interest in reducing nutrients in ground and surface waters that discharge into the Bay, particularly from fertilizer used on agricultural fields, have led to the development of best management practices (BMP), such as riparian forest buffer systems (RFBS). RFBS involve planting trees along waterways to mitigate nutrients in ground water and runoff before it is discharged into receiving waters (Jordan et al., 1997). In Maryland, past successes in planting buffers can be partially attributed to the implementation of a 1997 statewide program under the national Conservation Reserve Enhancement Program (CREP). CREP provides incentives to farmers to plant RFBS to reduce nutrient pollution in streams and rivers. A 2012 CREP Annual Report by Maryland Department of Natural Resources (MDDNR) estimated reductions of 8 million pounds of nitrogen (N), 760 thousand pounds of phosphorus (P), and 138 thousand tons of sediment due to 69,000 acres of land enrolled in CREP and converted into RFBS statewide (DNR, 2014). While these calculated reductions were estimated from studies that examined nutrient uptake by RFBS in various physiological provinces, such as the Coastal Plain, Piedmont, Ridge and Valley (R&V), and Appalachian Mountains, only a few studies have been performed in the R&V and Appalachian Mountains to support these estimates of nutrient reduction (Jacobs & Gilliam, 1985; Messer et al., 2012; Snyder et al., 1998). In most cases, statistical models are found most reliable when applied to the Coastal Plain, but not in other regions (Weller et al., 2011).

The efficacy of RFBS for nutrient retention is thought to be controlled by a variety of factors governing the hydrological interactions between surface water and adjoining groundwater and hyporheic environments (e.g., soil type; local hydrogeological conditions; groundwater residence time; water table depth; and topography/slope), as well as the particular characteristics of the buffers themselves (e.g., species planted, survival rate, density, age, etc.) (Bohlke and Denver, 1995; Gold et al., 1998; Hill, 1996; Lowrance et al., 1997; Schoonover and Williard, 2003)). Many of these factors are likely to vary dramatically between the R&V and the Coastal Plain, as well as among watersheds within the R&V province where this study was conducted. The research funded by this grant focused on assessing the hydrogeologic controls on RFBS functions within the R&V physiographic province through a field investigation conducted in four Potomac River sub-watersheds. The overall goal of the project was to determine if RFBS significantly enhance stream water quality in these four systems by decreasing loads and concentrations of nutrients discharging to surface waters.

B) Objectives

The specific objectives of this research project were to:

- characterize the spatial variation in stream discharge, stream water nutrient concentrations, and loads within and among four basins in the Ridge and Valley province;

- determine the spatial variation in the direction and magnitude of lateral groundwater discharging to the mainstem of the four streams;
- quantify the dominant sources of streamflow and nutrient loads (i.e., diffuse lateral groundwater, springs, and tributaries) under baseflow conditions;
- determine whether the distribution of nutrient loads in lateral groundwater discharging to the streams is correlated with the presence (or absence) of RFBS along the four study reaches; and
- examine how the interactions between surface water and shallow groundwater within a representative buffered reach vary temporally over a six-month time period.

II) Methods

A) Synoptic Study

A synoptic field investigation of groundwater-surface water interactions was conducted in four watersheds located within the R&V province of western Maryland. This investigation addressed research objectives 1 through 4 and focused on spatial variations in nutrient loads and their relationship to RFBS under seasonal baseflow conditions during the period from spring 2016 through spring 2017.

i) Study watersheds

The first watershed selected is located in Allegany County near Flintstone, Maryland: Murleys Branch watershed (MB; area=32 km^2) is a subwatershed of Town Creek watershed. The other three watersheds are located in Washington County near Hagerstown, Maryland and are subwatersheds of the Antietam Creek watershed. The three selected sub-watersheds within Antietam Creek watershed include Beaver Creek (BC; area= 87 km^2), Little Antietam Creek North (LACN; area=64 km^2), and Little Antietam Creek South (LACS; area=83 km^2). The four watersheds were selected because they each contain relatively large numbers of CREP participants who implemented RFBS as BMPs to reduce stream nutrient levels and some of the stream reaches within each watershed were studied in conjunction with a previous research project partnered with Department of Natural Resources (DNR) and The Nature Conservancy (TNC). During our previous research, we had found that some of these streams were "losing reaches". Resampling enabled us to further test if the hydrological characteristics (such as being a "losing reach") impacts the function of RFBS and to verify if these characteristics are consistent over time. Our selection of the Antietam Creek subwatersheds also stemmed from a report published in 1996 which found that the mainstem and its tributaries were not meeting Maryland's water quality standards for sediments, dissolved oxygen, and nutrients, thus the stream was classified as "impaired" (USEPA, 2015). Therefore, our research was designed to help assess how well RFBS are actually able to mitigate nutrient pollution in R&V streams where organizations are relying on these BMPs to improve water quality.

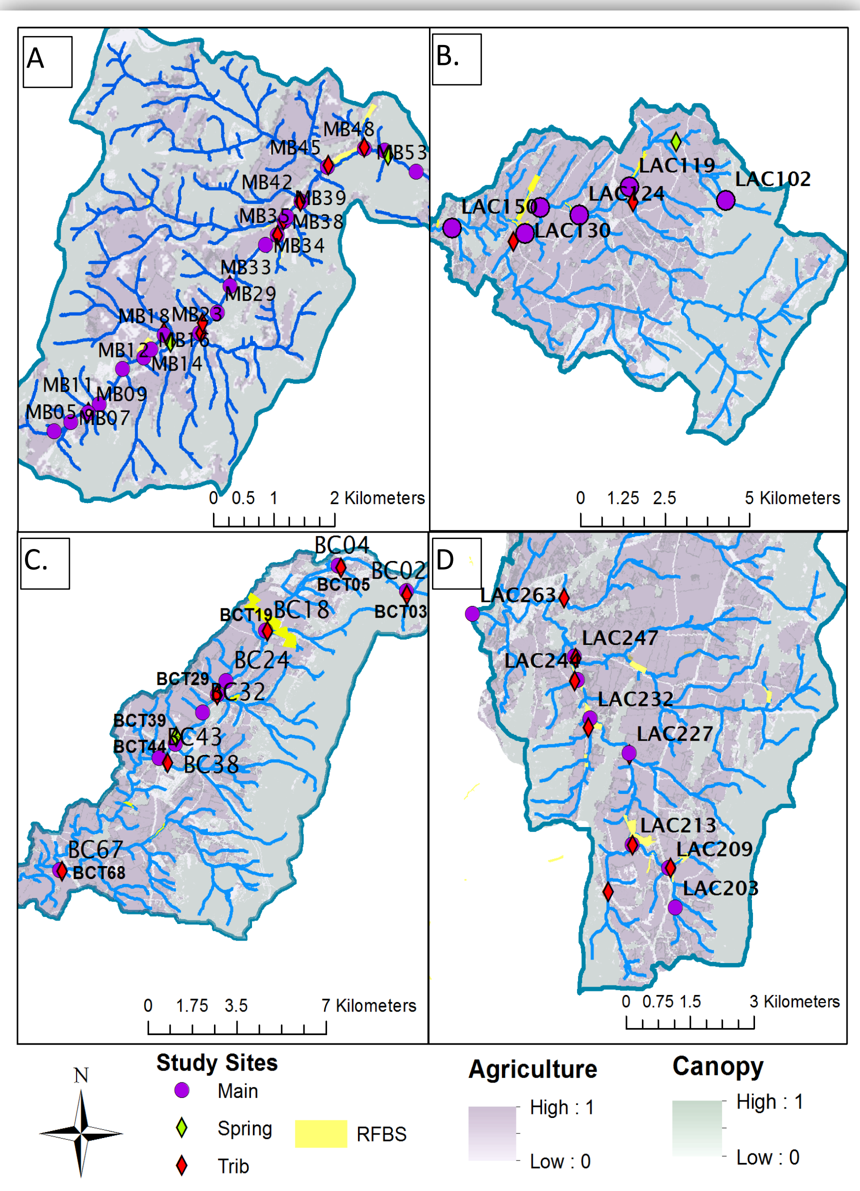

Figure 1 Maps showing locations of the synoptic study sites within the four R&V study watersheds: (A) Murleys Branch, (B) Little Antietam Creek North, (C) Beaver Creek, and (D) Little Antietam Creek South.. Planted buffers are represented by yellow polygons along the streams and canopy cover and agriculture are represented by green and purple color ramps, respectively. All four watersheds are located in regions containing carbonate geology and karst.

Each of the four watersheds has a similar land use layout with forest dominating the upland portion of the basin and the lower valleys and riparian areas dominated by cropland (Figure 1). A total of 24 farmers were identified as participating in CREP projects within these watersheds. Table 1 provides an overview of RFBS in each watershed, including the number of CREP participants, percentage of total contributing area dedicated to RFBS, percentage of streams buffered within the entire watershed, range and average year of RFBS planting, and range and average of canopy cover for each RFBS (statistics of RFBS were found using 'Zonal Statistics as Table' tool in ArcGIS). Based on an overlay of the canopy cover and planted buffer GIS layers, we found that MB has the highest percentage of stream buffering (11%), but the lowest average percentage of canopy cover associated with the planted buffers (35%). BC has the highest average of planted buffer canopy cover (49%), followed by LACS (47%), and LACN (39%).

LACS was found to have the most CREP participants (10), but only 9% of the stream network is buffered. About 5% of the stream network within both BC and LACN watersheds is buffered. The mean RFBS planting year was similar among the four watersheds (i.e., 2001 or 2002).

The four watersheds also vary to some degree with respect to land use and hydrological characteristics. MB contains 74% mixed forest, 22% agriculture (hay/grass/pasture/corn), and 4% rural residential (USDA, 2016). Two large springs are known to discharge into the MB mainstem (Murleys Branch Spring and Warm Spring). Additional smaller springs have also been observed throughout the sub-watershed during sampling times. Flintstone Creek, a neighboring tributary separated by a mountain, also upwells into MB by following an underground flow path that eventually surfaces and merges with MB just upstream of the Warm Spring tributary. Deciduous forest dominates the land use in the three Washington County watersheds (BC: 44%; LACN: 40%; and LACS: 36%), followed by grass/pasture (BC: 17%; LACN: 23%; and LACS: 23%). Corn is the dominant agricultural crop in BC and LACN (9% and 10%, respectively), while other hay/non-alfalfa is dominant in LACS (9%). Corn makes up 7% of the LACS watershed (USDA, 2016). Each of the Antietam Creek sub-watersheds contains springs as well. Beaver Creek has one of the largest springs in Maryland with an average discharge of 11,000 L/min (Seneca Valley Trout Unlimited, n.d.); the spring is the main source of water for the Albert Powell Hatchery located near Hagerstown.. Two unnamed springs were identified in LACN during sampling and while we did not discover any springs in LACS, it is assumed that we mislabeled some as tributaries, which is also likely for the other watersheds as well.

Table 1 Riparian Forest Buffer System (RFBS) data for each watershed (Murleys Branch- MB; Beaver Creek- BC; Little Antietam Creek North- LACN; and Little Antietam Creek South – LACS)

Sub-watershed	Total # of CREP Participants	Percent RFBS per Total Contributing Area	Pecent of stream buffered	Range of years RFBS were planted	Average Year RFBS were planted	Range of Percent Canopy Cover within each RFBS	Average percent of Canopy Cover in RFBS
MB	5	1%	11	2000-2007	2002	9-50%	35%
BC	5	1%	5	2000-2003	2001	29-85%	49%
LACN	4	0.6%	5.5	1999-2004	2002	16-66%	39%
LACS	10	0.85%	9	1999-2003	2001	20-87%	47%

ii) Field Methods

We addressed research objectives 1, 2, 3, and 4 by conducting comprehensive, longitudinal, synoptic stream surveys under baseflow conditions during two spring seasons (2016 & 2017) and one fall season (2016) in each of the four watersheds. In order to ensure consistent hydroclimatological conditions during each survey, all sampling within each subwatershed was generally completed on the same day. Sampling locations (i.e., "stations") in each subwatershed were identified using a high-resolution stream map to locate springs and tributaries along the mainstem. "Instantaneous" wading stream discharge measurements were made 1) just below the upstream node of each mainstem reach (defined by its confluence with a tributary or major spring); and 2) near the downstream end of each tributary or spring discharging into the mainstem. Measurements were typically made (and samples collected) at the pre-selected stations; in some instances, measurements were taken at locations where there was more convenient access to the particular reach, however (i.e., at road crossings and other locations where we were able to acquire permission to access the stream from tenants or property owners). This approach allowed us to ensure completion of all sampling and measurements within each watershed in a single day. The synoptic survey portion of the study thus included a total of 74 stations (31 in MB; 17 in BC; 10 in LACN; and 16 in LACS).

Water velocity (0.6 times depth below the water surface) and depth measurements were made at 10-30 regularly-spaced intervals along a suspended tagline using a Marsh-McBirney digital electromagnetic current meter attached to a top-setting wading rod. Total instantaneous discharge at each station was computed using the mid-section method. Net (instantaneous) lateral groundwater discharge (to each reach i: $Q_{lat(i)}$) was computed as the difference between the discharge measured at the upstream node of the reach below reach i (assumed equal to $Q_{D(i)}$) and the sum of the discharge measured at the upstream node of reach i ($Q_{U(i)}$) plus the discharge (if any) from the corresponding tributary ($Q_{T(i)}$) or spring (Q_s). Negative computed values of $Q_{lat(i)}$ were thus indicative of a losing reach, although for some purposes we required that $Q_{lat(i)}$ exceed a certain percentage of Q_D for us to consider a particular reach as "losing". For instance, if the reach was found to be gaining after incorporating 5% error in the flow discharge calculation, the stream was relabeled as "indefinite".

Water samples (i.e., "grabs") were collected at each of these stations in 1L polyethylene cubitainers, immediately placed on ice in a cooler, and transported to our analytical laboratory in Frostburg where they were filtered (0.45 μm), aliquoted, preserved, and analyzed for nutrients (TDN, TDP, PO_4-P, NH_3-N, NO_2-N, NO_3-N, and dissolved organic nitrogen (DON)) using a Lachat flow injection analyzer (FIA). Filtered aliquots of each sample were also analyzed for major ions (chloride: Cl^-; bromide: Br^-; sulfate: SO_4^{2-}; calcium: Ca^{2+}; magnesium: Mg^{2+}; sodium: Na^+; and potassium: K^+) by ion chromatography (anions) and atomic absorption/emission spectroscopy (cations), as well as for conductivity (meter); acid neutralizing capacity (ANC) by automated acidimetric Gran titration; and dissolved organic carbon (DOC) by UV-assisted persulfate digestion. Major ion concentrations were used to test our methodology for identifying losing and gaining reaches by employing a steady-state reach mass balance model for biologically-conservative constituents. Dissolved silica (Si) concentrations were also measured by FIA on samples collected during the fall 2016 and spring 2017 surveys to further test our methodology.

A 10-meter digital elevation model (DEM) and an ArcGIS watershed delineation tool were used to delineate sub-watersheds and estimate total contributing area (TCA) and local contributing area (LCA) for each study reach. The eco-hydrologically active (EHA) area (or riparian region) for each reach was defined with the help of our partner, Dr. Kathy Boomer from TNC, using high resolution topography data to map wetland, stream, and river morphologies near-surface ground and surface-water interactions. Dr. Boomer combined topographic derivatives, including open water, headwater, riparian, and floodplain wetlands, and incised streams. A high-resolution stream map was developed using DEM's with 1 to 2 m pixel resolutions using LiDAR. EHA areas were identified using an assumption that perennial surface water features represent location of a high water table (Winter et al., 1998) and that areas with surface elevations within 1.5 m of the nearest perennial water feature have the greatest probability of having a shallow water table conducive to biogeochemical processes. The EHA area was then intersected with the National Land Cover Dataset (produced by the MRLC) (Homer et al., 2015) to calculate the areas of forested (FEHA) and non-forested EHA (NFEHA), canopy cover, and area in cultivated agriculture within each subwatershed. The Cropscape data layer (USDA, 2016) was used to identify specific agricultural land uses; planted buffer shapefiles were based on Landsat imagery and site information acquired from MDDNR.

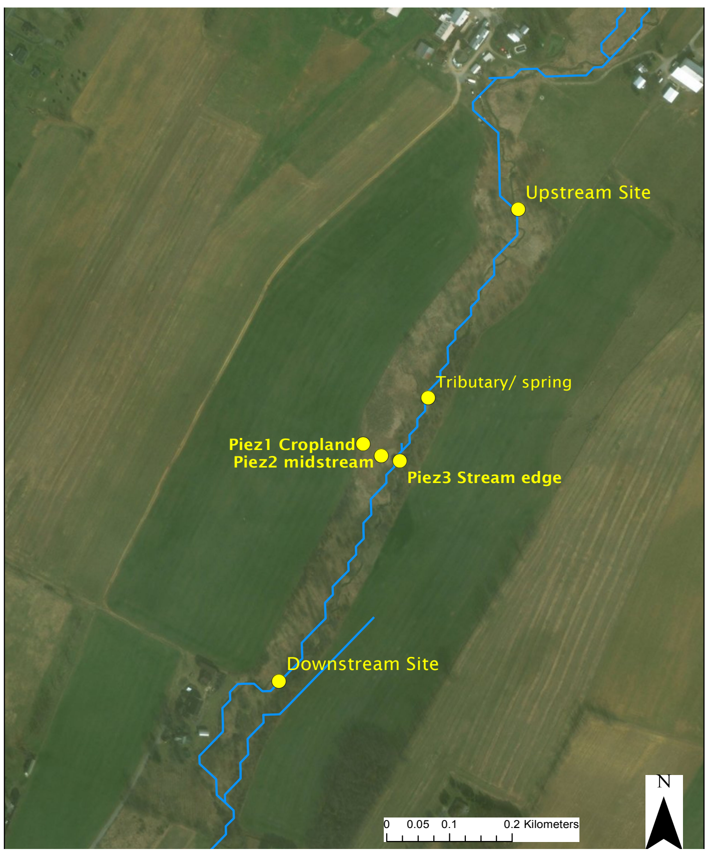

Figure 2 Map of intensive site located in Antietam Creek North from synoptic study within Washington County. Site contained a riparian buffer adjacent to an agricultural field. Aerial view shows piezometer transect within the middle of the buffer, along with upstream, downstream, spring, and mid- stream locations in yellow.

iii) Modeling

A steady-state stream network-mixing model, based on the fundamental principle of conservation of water and dissolved mass, was used to predict the variations in concentrations of dissolved constituents along each mainstem during each synoptic survey. For each reach i, the steady-state water balance equation can be written as:

$$Q_{D(i)} = Q_{U(i)} + Q_{T(i)} + Q_{S(i)} + Q_{lat(i)} \quad [1]$$

where Q is volumetric discharge and the subscripts D, U, T, S, and lat refer to downstream, upstream, tributary, spring, and net lateral inflow, respectively. Assuming a conservative behavior for a particular dissolved constituent, the corresponding mass balance equation is written as follows:

$$Q_{D(i)}C_{D(i)} = Q_{U(i)}C_{U(i)} + Q_{T(i)}C_{T(i)} + Q_{sS(i)}C_{s(i)} + Q_{lat(i)}C_{lat(i)} \quad [2]$$

where C is the concentration of the respective dissolved constituent. We explored the utility of two different mixing models: (1) a “base model”; and (2) an “actual flows” model. The “base model” used only the measured concentration data and assumed that the discharge at each station was directly proportional to the corresponding TCA obtained through subwatershed delineation (in effect, the corresponding TCA’s can be substituted for the Q’s in equations [1] and [2]). The “actual flows” model made use of both the measured concentration and field discharge data. Since $C_{D(i)}$ was measured in the field and $Q_{D(i)}$ was measured in the field (or could be estimated using the respective TCA in the base model), the model was employed to estimate $C_{lat.}$. Rather than using the model to estimate $C_{lat(i)}$ for each reach, we used the model to estimate the mean concentration of C_{lat} across each watershed such that the sum of squares of the differences between predicted and observed concentrations of each constituent in each reach was minimized. The model was implemented in Excel and optimized solutions were obtained using a customized Excel Solver routine and use of a Nash-Sutcliffe efficiency (E) (Nash & Sutcliffe, 1970).

B) Intensive Study

i) Study Site

We addressed objective 5 by examining the flow of shallow groundwater through the riparian region of a specific stream reach located in LACN watershed; this reach flows through a planted (2002 under CREP) RFBS that is about 60 meters wide (Figure 2). During the synoptic survey, we identified a large spring along Watery Lane that apparently supplies much of the water to this particular reach. The stream reach is about 425 meters long with a LCA of 0.59 km^2. The area between the cropland and stream within which we placed a piezometer transect is 0.067 km^2 with the entire area containing a RFBS. The soil in the riparian area is 84% Lindside silt loam, where a typical profile is silt loam until 1.7 meters depth, then gravelly sandy clay loam until about 2 meters depth. The parent material is loamy alluvium derived from limestone-sandstone-shale. It is moderately well-drained and the depth of the water table is about 0.5 m to 1.0 m below the ground surface (Soil Survey, 2017).

The adjacent agricultural field is presently managed using a soybean-wheat-corn crop rotation system, making up about 45% of the 0.59 km^2 watershed (Figure 3A). About 40.5% of the LCA contains grass/pasture and 7.2% is deciduous forest. In March 2017, wheat was planted and 70 pounds of N fertilizer per acre were applied at the time of planting. No additional fertilizer was applied thereafter. Soybeans were planted and grown in the field throughout the summer season as a double cropping system (D. Herbst, personal communication, Oct. 9, 2017).

ii) Field Methods

Upstream, downstream, and mid-section locations along the study reach were instrumented and monitored approximately biweekly between May 2, 2017 and November 1, 2017 under both baseflow and stormflow conditions. Staff gauges and Hobo water level loggers were installed and used to monitor gauge height (15-minute intervals) at each station using established USGS gauging methods (Figure 3B). Upstream and downstream biweekly discharge measurements were made in order to develop a rating curve for each station. Flow measurements and water samples were also collected from a very small spring in this watershed, located between the upstream site and piezometer transect. Surface water "grab" samples were collected at the three locations on a bi-weekly basis and handled/analyzed identically to the synoptic samples. A transect of three shallow piezometers was installed within the alluvial sediments near the mid-section of the reach to characterize the direction of shallow groundwater flow and the horizontal hydraulic gradient across the RFBS; boreholes for each piezometer were drilled using a handheld augur, and casings were

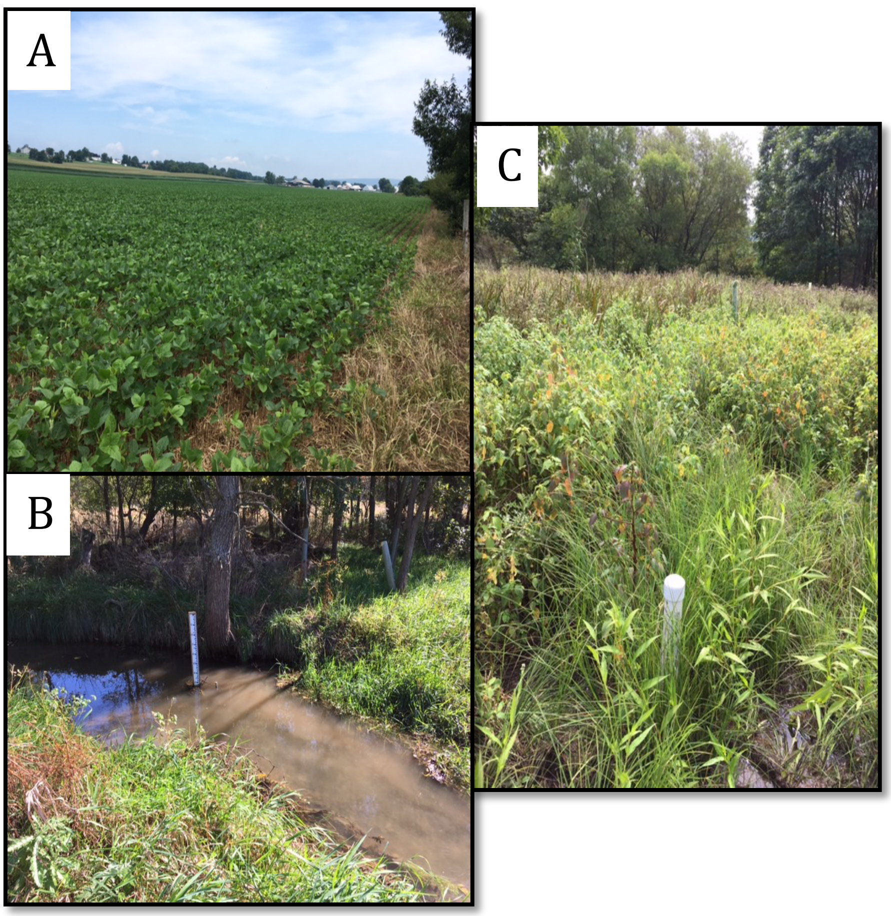

Figure 3 (A) Upland agricultural field growing soybeans, adjacent to the RFBS. (B) Staff gauge in downstream region of the reach. Upstream, downstream, and midstream stations each contained pressure transducers that were used to record water levels and temperatures at 15-minute increments. (C) Piezometer transect in vegetated area of buffer that were sampled biweekly for manual water level measurements and groundwater nutrient concentrations. Each piezometer contained pressure transducers reading at 15-minute increments.

constructed using 2” dia. schedule 40 PVC pipe, an endcap, a coupling, and a 12” section of 2” dia. PVC well screen. One piezometer was installed near the edge of the adjoining agricultural field, a second was installed approximately midway between the field and the stream (Figure 3C), and a third was installed on the streambank. Piezometers were installed to the depth allowed by bedrock, ranging from a 1.2 to 3 meters below the ground surface.

On each sampling date, the depth to water below the top of the well casing was measured using a handmade water level measuring device comprised of two wires mounted in parallel to a 4’ section of ¾” dia. PVC pipe demarcated using an attached graduated (in mm) adhesive tape; the electrical wires were used as inputs to a digital multitester set to measure a resistance response when the wires contacted the free water surface in the piezometer. Piezometer (top of casing) elevations and locations were surveyed relative to a temporary benchmark using an engineer’s level, tripod, stadia rod, and field measuring tape. Following surveying, all depth to water readings were converted into units of hydraulic head (m) relative to the approximate elevation of the temporary datum (~800 ft). Hobo water level loggers were installed in each piezometer to provide a continuous time series of 15-minute readings. “Grab” groundwater samples were collected from each piezometer using a PVC bailer after one complete volume had been displaced (Clement et al. 2003; Messer, 2012). Groundwater samples were handled and analyzed using the identical methods employed in the synoptic studies.

III) Principal Findings

A) Synoptic Study

Our first objective was to characterize the spatial variation in stream discharge along each mainstem of the four watersheds. Our null hypothesis was that stream discharge increases proportionally with total contributing area, but we expected to observe significant variability attributable primarily to the various springs located throughout these watersheds. To test this hypothesis using the field data, we developed linear models (Eq. [3]) between mainstem discharge and TCA based on mean daily discharges for our sampling dates reported by USGS for downstream gauges on Town Creek and Antietam Creek:

$$Q_j = \frac{Q_{USGS}}{TCA_{USGS}} * TCA_j \qquad [3]$$

where Q_{USGS} and TCA_{USGS} are the measured mean daily discharge and total contributing area (i.e., watershed area) reported by USGS, respectively; and TCA_j is the total contributing area associated with each mainstem sampling station.

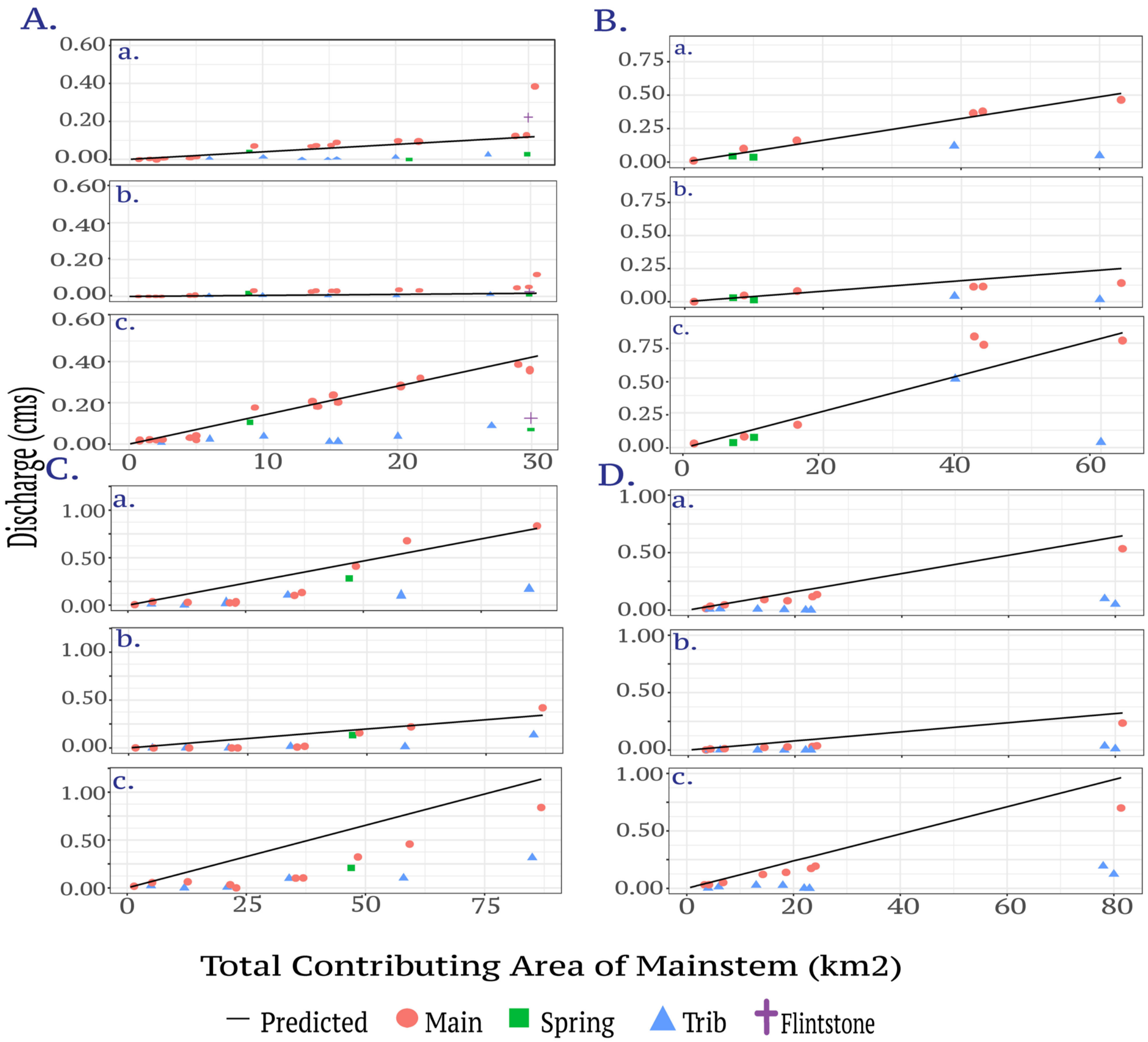

Figure 4 Measured discharge of the mainstem, spring, tributaries, and Flintstone Creek (MB only) as a function of total contributing area (TCA) for each watershed. Graphs illustrate how measured and predicted stream discharge varies as a function of TCA across four watersheds. (A.) is Murleys Branch (MB), (B.) is Little Antietam Creek North (LACN), (C.) is Beaver Creek (BC), and (D.) is Little Antietam Creek South (LACS). The (a.), (b.), and (c.) indicate the different seasons the measurements were taken (a. = spring 2016; b. = fall 2016; c. = spring 2017). Black linear line represents predicted discharge based on watershed area using USGS local stream gauge. TCA of the springs, tributaries, and Flintstone Creek (MB only) were manipulated to show where they are located along the mainstem; therefore, the x-axis are TCA's for the mainstems only.

Our results show that some sites from the mainstem were close to the predicted discharge rates. Using Nash-Sutcliffe Efficiency (NSE), the measured discharge was closest to the predicted discharge rates in MB in spring 2017 (NSE = 0.83), LACN in spring 2016 & 2017 (NSE = 0.94 and 0.84, respectively), BC in spring and fall 2016 (NSE = 0.72 and 0.62, respectively), and spring 2016 and 2017 for LACS (NSE = 0.83 and 0.74, respectively) (Fig. 4: A-c; B-a,b; C-a,b; D-a,b,c, respectively). Where there is a large increase in discharge, it is anticipated to be a contribution from a spring, such as MB spring 2016 (Fig. 4A-a) and where discharge is less than expected, we expect the stream is losing water along the mainstem, such as BC in spring 2017 (Fig. 4C-c). In some of these instances, we are aware of the location of springs, such as in MB, but because we were unable to identify all springs along the mainstem for each of the subwatersheds, we can infer where springs are present when mainstem discharge is higher than the linear model predicts.

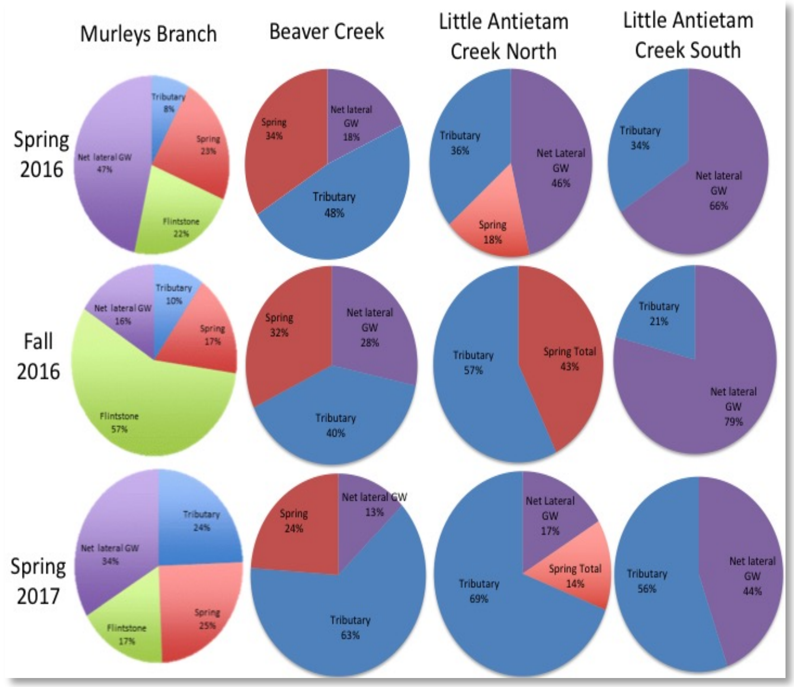

Figure 5 Pie charts illustrating the distribution of direct sources of baseflow to the mainstem of each of the four studied watersheds during three seasons (spring 2016, fall 2016, and spring 2017). Note: since not all springs were identified, it is likely that we have underestimate the spring contributions.

We also used the synoptic field discharge data to address objective 3 (i.e., to quantify the primary contributions of different water sources to the mainstems and understand how these sources influence stream water quality). Figure 5 shows the distribution of direct sources (i.e., net lateral groundwater, tributaries, and springs) for each of the four watersheds during the three sampled seasons. Distribution estimates were based on the actual discharge measurements made in the field. Spring contributions were likely underestimated because not all springs were identified and some tributaries may be influenced by upstream springs. Similarly, tributary discharges also likely include significant lateral groundwater flow that could not be resolved using our field methodologies. During the 2016 spring seasons, lateral groundwater was the dominant, direct contributor of flow to the mainstems in MB, LACN, and LACS, but in fall 2016, only LACS was still dominated by direct discharge of lateral groundwater. Direct discharges from springs were significant, but not dominant, contributors in MB, BC, and LACN during all three sampling periods, but insignificant in LACS. The current paradigm of nutrient filtering by RFBS suggests that buffers planted in riparian zones will be most effective in locations where lateral groundwater is the predominant water source to a reach and where there is a hydrologic connection between the nutrient source, the buffered area, and the stream (Lowrance *et al*., 1997). This would also potentially include LACS during the fall season and MB during the spring 2017 season. However, we did not find significant results to support this hypothesis. It should be emphasized that our interpretations of these data are based on the aggregation of water sources relative to the outlet of each mainstem reach; our methodology also allows for an assessment of water sourcing for individual mainstem reaches within each basin (i.e., objective no. 2)—an important area of our on-going research in these basins.

We also used the synoptic data to determine whether the distribution of nutrient concentrations and loads in lateral groundwater discharging into the stream is correlated with the presence (or absence) of RFBS along the four study reaches. Although analyses were performed for all constituents that were measured, we focused only on concentrations and loads of TDN, TDP, and SO_4 for this report. SO_4 was selected because it can help discern how the stream water chemistry changes along the mainstem depending only on the contributing sources (i.e., lateral groundwater, tributaries, and springs) without the influence of biological transformations. Additionally, it is also found naturally in groundwater from the breakdown of rocks and soils (Solomon et al., 2009) and atmospheric S deposition; and SO_4 concentrations are not influenced by winter road salt that is used in Maryland, unlike sodium chloride (MDOT/SHA, 2017). Figure 6 shows the variation of TDN (I), TDP (II), and SO_4 (III) along the mainstem along with locations of RFBS (shown by the green, transparent background). TDN concentrations decreased slightly where RFBS were present along the mainstem in MB and BC watersheds, but LACN and LACS did not show such distinct declines (Figure 6, I.-A, C, B, and D, respectively). These observations suggest that TDN concentrations are not universally influenced by the presence of RFBS, rather by the water quality of the tributaries and springs that make up the majority of the mainstem discharge. TDN concentrations showed similar patterns among the spring and fall seasons in all four watersheds, despite the lower expected rates of nutrient retention in the fall after leaf abscission had begun, evapotranspiration had decreased, and rates of biological activity would likely be lower due to lower temperatures. Where reaches were clearly losing water (or where the direction of net lateral groundwater flow was considered indefinite), TDN concentrations sometimes increased in the downstream direction when we expected them to remain steady. Our results thus highlight the greater significance of nutrient inputs from springs and tributaries, similar to results reported by Bohlke *et al*. (1995) for a watershed near Locust Grove, Maryland showing that nutrient concentrations in streams depended primarily on discharges from deeper aquifers containing older waters.

TDP concentrations in the mainstem of MB showed a slight decline where RFBS were present in all three sampling dates (Figure 6, II.A). LACN and LACS showed some variation that again appear to be better explained by spring and tributary contributions than by presence/absence of RFBS (Figure 6, II- C and D, respectively). BC had the greatest variation in TDP concentrations throughout the mainstem and among the different sampling dates (Figure 6 II. B). One particular BC station showed a dramatic increase in TDP in fall 2016 (~35 km^2 TCA), even with the presence of a RFBS and loss of surface water. This is most-likely due to the high concentration of TDP within the tributary being discharged into the stream. However, during spring 2017, TDP concentrations in the mainstem exceeded the tributary concentration and the reach was receiving waters from baseflow lateral discharge. SO_4 concentrations in BC showed the same pattern during fall 2016 (Figure 6, III.C.b). The tributary had a much lower concentration, indicating that the SO_4 and TDP concentrations increased due to the high concentrations in lateral groundwater or from an unidentified spring.

SO_4 concentrations in the mainstems of MB, LACN, and LACS each showed patterns that could be explained by contributing tributaries and springs (Figure 6, I.A/C/D) for all three sampling dates, except LACS where tributaries were dry during the fall season (~20 km^2). Concentrations still declined, however, similar to the pattern observed on the other two sampling dates.

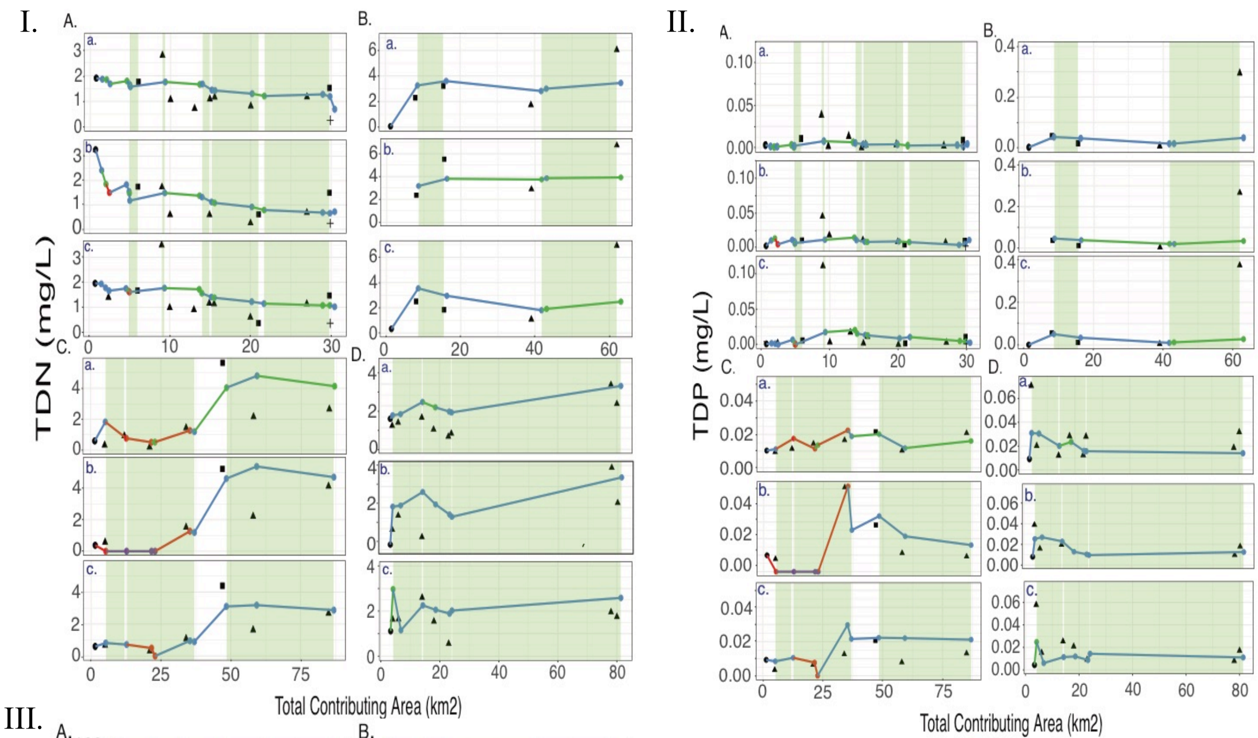

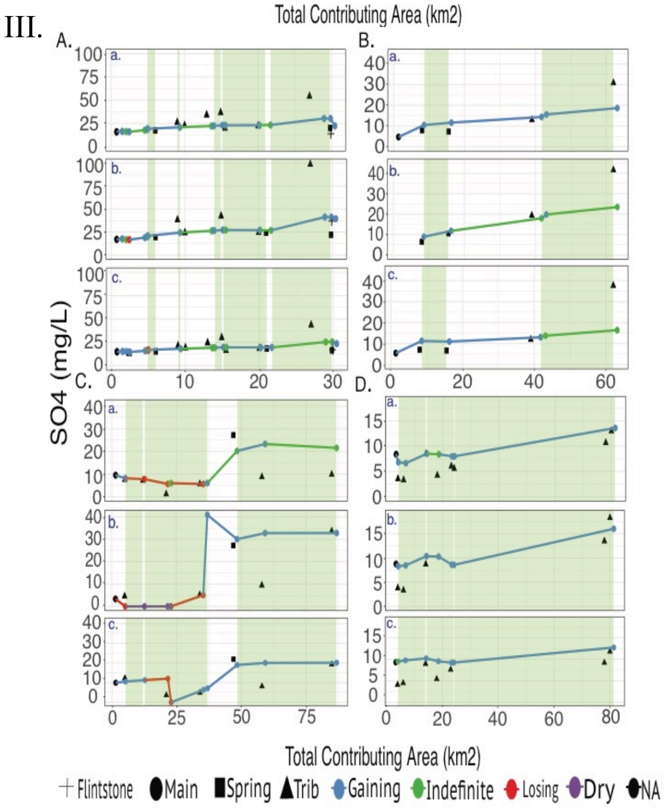

Figure 6 (I) Total dissolved nitrogen (TDN), (II) total dissolved phosphorus (TDP), and (III) sulfate (SO4) in mg/L along the mainstem, from upstream to downstream as the total contributing area (TCA) on the x-axis increases further downstream. (A.) is Murleys Branch (MB), (B.) is Little Antietam Creek North (LACN), (C.) is Beaver Creek (BC), and (D.) is Little Antietam Creek South (LACS). The (a.), (b.), and (c.) indicate the different seasons the measurements were taken (a. = spring 2016; b. = fall 2016; c. = spring 2017). Measurements taken along the mainstem are connected by line segments to show more clearly the variation within all of the watersheds. The line colors represent the state of the stream (i.e., dry, gaining, losing, indefinite). Because some of the losing streams were very close to being either positive or negative with a 5% calculated error, those were labeled indefinite. Watershed area of springs and tributaries were modified to represent their location/ contribution to the mainstem on the graph. Green transparent background indicates location of buffers along the mainstem.

Finally, we applied the steady-state stream network mixing model to the problem of characterizing spatial variations in stream water nutrient concentrations and loads (TDN, TDP, and SO_4) within and among the four basins in the R&V province., Two versions of the model were employed: a “base model” and an “actual flows model” (described in Methods section) with optimal solutions based on minimizing errors using a Nash-Sutcliffe model efficiency coefficient (E). Modeling results are presented in Figures 7, 8, and 9, with root mean square errors (RMSE, E values, and predicted constant mean (C_{lat}) concentrations found in the tables underneath each graph. The modeling results suggested that the “actual flows model” was superior to the base model in predicting mainstem TDN concentrations for all three sampling dates for BC, but only for the spring seasons for MB and spring and fall 2016 for LACN. BC concentrations were the most difficult to predict because the reach was either dry or had lost surface water, making the actual measured discharge necessary when predicting nutrient concentrations. The “base models” predicted TDN variations in LACS best where the majority of the mainstem contained gaining reaches and had consistently, large contributions from lateral groundwater. However, the “base model” was also a better predictor of TDN in the fall season in MB and spring 2017 season in LACN where net lateral groundwater either had little or no contribution. In most cases, predicted C_{lat} values for both models were between the observed ranges; however, there were a few instances where C_{lat} was over-estimated, including the C_{lat} value that was used in the “actual flow model” used to predict TDN spring 2017 concentrations in LACN and the base model for spring 2017 in LACS.

TDP was much more difficult to accurately predict using the mixing model because of the very low observed concentrations, resulting in the models using very low C_{lat}. Based on a lower RMSE and higher E, the “actual flows model” for all three sampling dates for MB and LACN and fall 2016 and spring 2017 for BC worked best in predicting TDP. Again, predicted C_{lat}’s were within the observed ranges for most of the subwatersheds, excluding only a few, including: MB during spring 2016, where TDP was underestimated by the “actual flow model”; LACS during both spring seasons, where the “base model” underestimated TDP; and in LACN during spring 2017 where the “actual flow model” overestimated TDP. Underestimation seemed to occur when the highest concentrations of TDP were in the upstream sites where discharge was low and then again at the most downstream sites where discharge was greatest. In the mid-section of the mainstem, concentrations were lowest, even as flow rate increased. Therefore, to compensate, the constant C_{lat} was lower than the average observed concentration. Overestimation occurred when the upstream sites with smaller discharges again contained high concentrations, but were much higher than all of the downstream sites that had the highest discharge rates. Therefore, the model seems to over-predict to accommodate sites that have a high TDP concentration, but low flow rates.

Combining results of TDN and TDP, the “actual flow model” remained to be the superior model. We found that each watershed was unique when quantifying the main contribution of water sources to the mainstem; therefore, suggesting that the “base model” will most-likely work best when groundwater is the predominant source of the mainstem and discharge rates can be estimated using TCA. Of the four watersheds, we found LACS matched the closest to this description, which the “base model” did work best for predicting TDN and TDP for all three sampling dates. Therefore, the accuracy of the model most-likely depends on the hydrology of the watershed. However, TDN and TDP can be converted into different chemical forms depending on the environment and susceptibility to biological uptake that could make predicting these constituents more challenging. Using a conservative constituent, such as SO_4 to further test the accuracy of the models without the influence of biological uptake, it was found that the “base model” worked best amongst all watersheds. This included: in MB for fall 2016 and spring 2017; LACN during fall 2016 and spring 2017; and all three sampling dates in LACS. Of these watersheds and sampling times, net lateral groundwater only had a large contribution in MB during spring 2017 and LACS during all three sampling dates. This further supports the hypothesis that the hydrology is complex within watersheds located in the R&V, that the “base model” only sometimes works well for watersheds that are dominated by lateral groundwater and consists mostly of gaining reaches, but there are a few exceptions. Additionally, based on the E values, the models did not do an overwhelmingly better job at predicting SO_4 when comparing to the results of TDN and TDP. Therefore, no matter what the constituent (conservative or not), it is difficult to predict nutrient and ion concentrations of streams located in the R&V because of the inherent hydrogeological complexity.

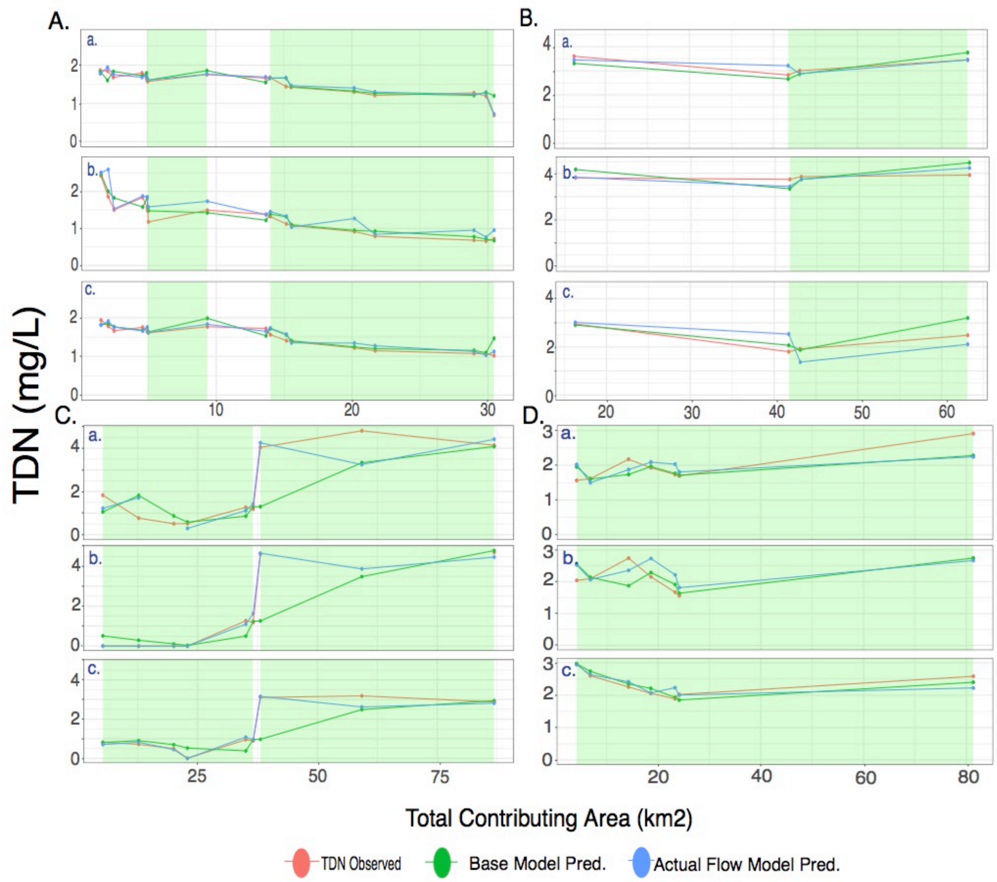

Figure 7 Graphs of observed (red) and predicted (green and blue), raw nutrient concentrations of TDN in baseflow groundwater as a function of Total Contributing Area (TCA) (km^2). "Base Model" (green) used the watershed area to predict a constant discharge into the stream that simulates baseflow, groundwater discharge as being proportional to the watershed area and containing a constant concentration of the nutrient (Clat). "Actual Flow Model" (blue) used measured discharge as well as the constant nutrient concentration (C_{lat}) to predict nutrient variations. Graph are the following sites: (A.) Murleys Branch, (B.) Little Antietam Creek North, (C.) Beaver Creek, and (D.) Little Antietam Creek South. Spring 2016, fall 2016, and spring 2017 plots are indicated by (a), (b), and (c), respectively.

Table 2 Results of Nash-Sutcliffe model efficiency coefficient (E), root mean square (RMSE), and predicted TDN constant concentration (Clat) for the "base model" and "actual flows model". Bolded results highlights results that support each model.

	Murleys Branch						Little Antietam Creek North					
	Spring16		Fall16		Spring17		Spring16		Fall16		Spring17	
	Base	Actual	Base	Actual	Base	Actual	Base	Actual	Base	Actual	Base	Actual
E	0.69	**0.91**	**0.87**	0.67	0.67	**0.87**	0.44	**0.49**	-0.61	**0.40**	**0.71**	0.01
RMSE	0.16	**0.09**	**0.17**	0.27	0.15	**0.10**	0.24	**0.22**	0.38	**0.22**	**0.38**	0.49
Clat	1.78	1.65	1.67	1.88	1.69	1.65	4.11	4.58	3.89	4.25	4.21	7.14
	Beaver Creek						Little Antietam Creek South					
	Spring16		Fall16		Spring17		Spring16		Fall16		Spring17	
	Base	Actual	Base	Actual	Base	Actual	Base	Actual	Base	Actual	Base	Actual
E	0.50	**0.78**	0.63	**0.94**	0.53	**0.97**	**0.45**	0.34	**0.38**	0.34	**0.87**	0.70
RMSE	1.18	**0.78**	1.39	**0.56**	0.85	**0.21**	**0.33**	0.36	**0.47**	0.49	**0.13**	0.20
Clat	1.87	1.96	0.55	1.99	1.04	0.86	2.57	2.29	3.68	2.68	3.92	3.02

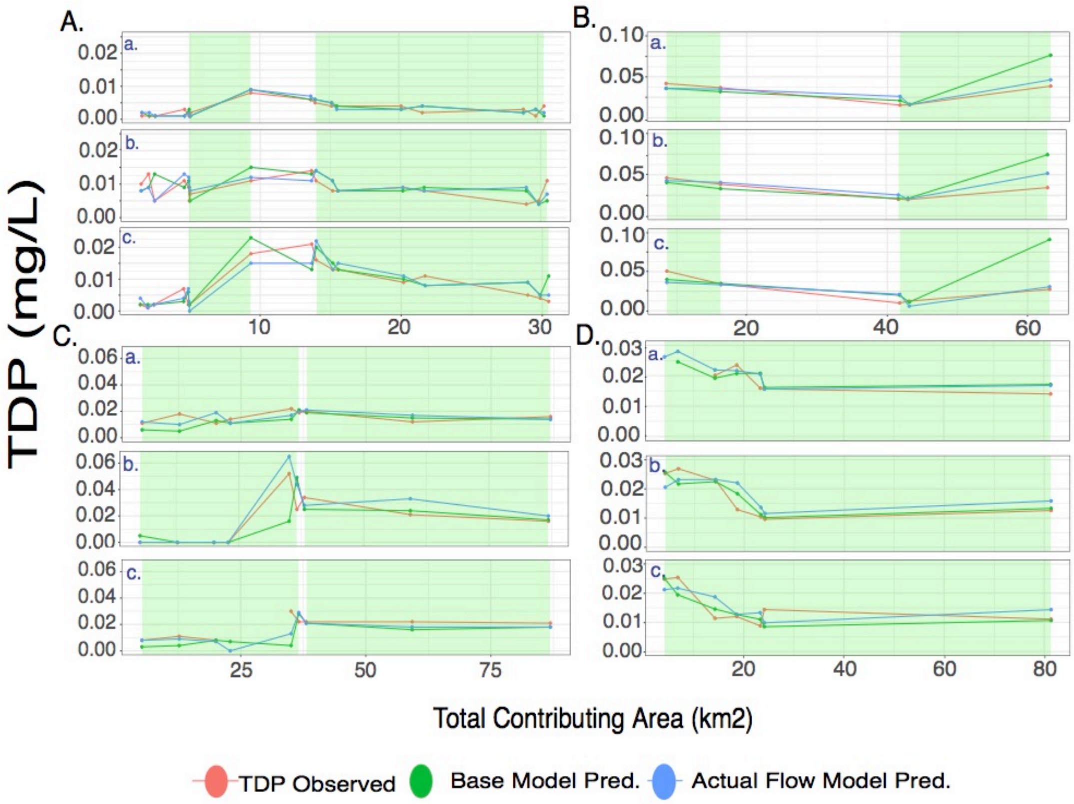

Figure 8 Graphs of observed (red) and predicted (green and blue), raw nutrient concentrations of TDP in baseflow groundwater as a function of Total Contributing Area (TCA) (km^2). “Base Model” (green) used the watershed area to predict a constant discharge into the stream that simulates baseflow, groundwater discharge as being proportional to the watershed area and containing a constant concentration of the nutrient (Clat). “Actual Flow Model” (blue) used measured discharge as well as the constant nutrient concentration (C_{lat}) to predict nutrient variations. Graph are the following sites: (A.) Murleys Branch, (B.) Little Antietam Creek North, (C.) Beaver Creek, and (D.) Little Antietam Creek South. Spring 2016, fall 2016, and spring 2017 plots are indicated by (a), (b), and (c), respectively.

Table 3 Results of Nash-Sutcliffe model efficiency coefficient (E), root mean square (RMSE), and predicted TDP constant concentration (Clat) for the “base model” and “actual flows model”. Bolded results highlights the results that supports each model.

	Murleys Branch						Little Antietam Creek North					
	Spring16		Fall16		Spring17		Spring16		Fall16		Spring17	
	Base	Actual	Base	Actual	Base	Actual	Base	Actual	Base	Actual	Base	Actual
E	0.54	**0.64**	-0.43	**0.19**	0.64	**0.77**	-1.26	**0.68**	-2.11	**0.43**	-2.80	**0.66**
RMSE	0.00	**0.00**	0.00	**0.00**	0.00	**0.00**	0.02	**0.01**	0.02	**0.01**	0.03	**0.01**
Clat	0.00	0.00	0.01	0.01	0.00	0.01	0.04	0.03	0.05	0.05	0.05	0.06
	Beaver Creek						Little Antietam Creek South					
	Spring16		Fall16		Spring17		Spring16		Fall16		Spring17	
	Base	Actual	Base	Actual	Base	Actual	Base	Actual	Base	Actual	Base	Actual
E	**-0.15**	-0.34	0.28	**0.75**	-0.15	**0.48**	**0.74**	0.78	**0.83**	0.57	**0.69**	0.53
RMSE	0.01	**0.00**	0.01	**0.01**	0.01	**0.01**	**0.00**	0.00	**0.00**	0.00	**0.00**	0.00
Clat	0.02	0.01	0.00	0.04	0.00	0.01	0.00	0.01	0.02	0.02	0.00	0.02

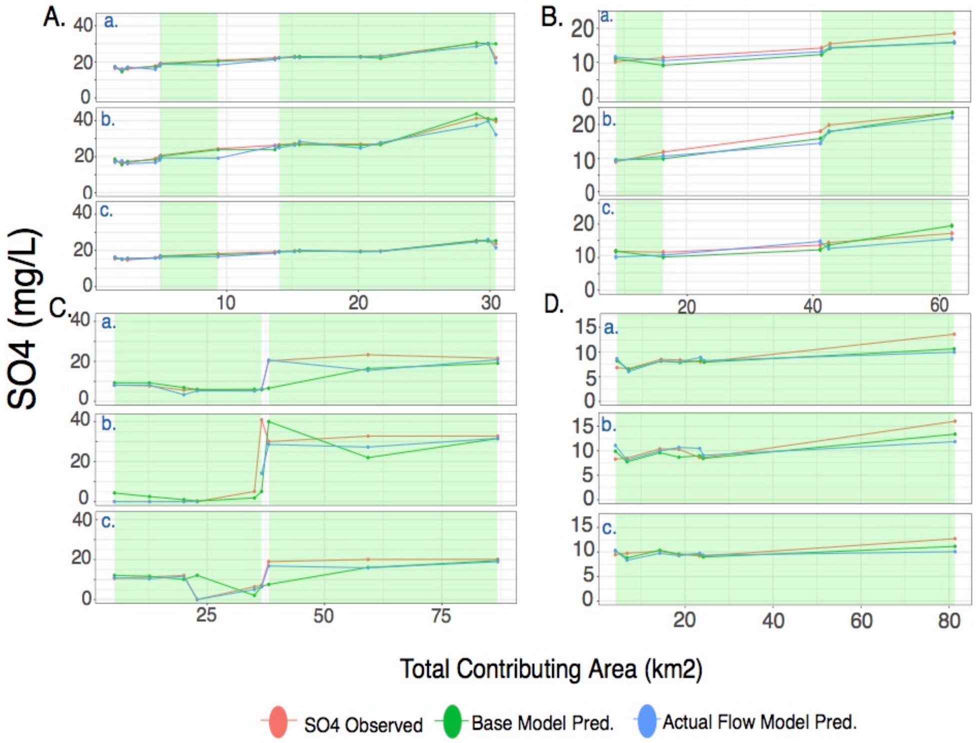

Figure 9 Graphs of observed (red) and predicted (green and blue), raw nutrient concentrations of SO_4 in baseflow groundwater as a function of Total Contributing Area (TCA) (km^2). "Base Model" (green) used the watershed area to predict a constant discharge into the stream that simulates baseflow, groundwater discharge as being proportional to the watershed area and containing a constant concentration of the nutrient (Clat). "Actual Flow Model" (blue) used measured discharge as well as the constant nutrient concentration (C_{lat}) to predict nutrient variations. Graph are the following sites: (A.) Murleys Branch, (B.) Little Antietam Creek North, (C.) Beaver Creek, and (D.) Little Antietam Creek South. Spring 2016, fall 2016, and spring 2017 plots are indicated by (a), (b), and (c), respectively.

Table 4 Results of Nash-Sutcliffe model efficiency coefficient (E), root mean square (RMSE), and predicted SO_4 constant concentration (Clat) for the "base model" and "actual flows model". Bolded results highlights results that support each particular model.

	Murleys Branch						Little Antietam Creek North					
	Spring16		Fall16		Spring17		Spring16		Fall16		Spring17	
	Base	Actual	Base	Actual	Base	Actual	Base	Actual	Base	Actual	Base	Actual
E	0.76	**0.91**	**0.98**	0.88	**0.96**	0.93	0.58	**0.72**	**0.91**	0.86	**0.53**	0.48
RMSE	2.00	**1.22**	**1.10**	2.69	**0.56**	0.87	2.07	**1.57**	**1.61**	1.99	1.51	**1.34**
Clat	18.85	18.20	20.35	16.81	16.72	17.89	13.33	17.12	11.96	14.51	13.13	25.17
	Beaver Creek						Little Antietam Creek South					
	Spring16		Fall16		Spring17		Spring16		Fall16		Spring17	
	Base	Actual	Base	Actual	Base	Actual	Base	Actual	Base	Actual	Base	Actual
E	0.48	**0.86**	0.39	**0.60**	0.16	**0.93**	**0.66**	0.45	**0.70**	0.36	**0.55**	0.15
RMSE	5.22	**2.75**	13.08	**10.64**	5.95	**1.72**	**1.26**	1.61	**1.39**	2.04	**0.77**	1.22
Clat	10.26	7.94	4.66	23.45	13.23	9.49	11.51	10.13	14.22	11.79	14.61	10.70

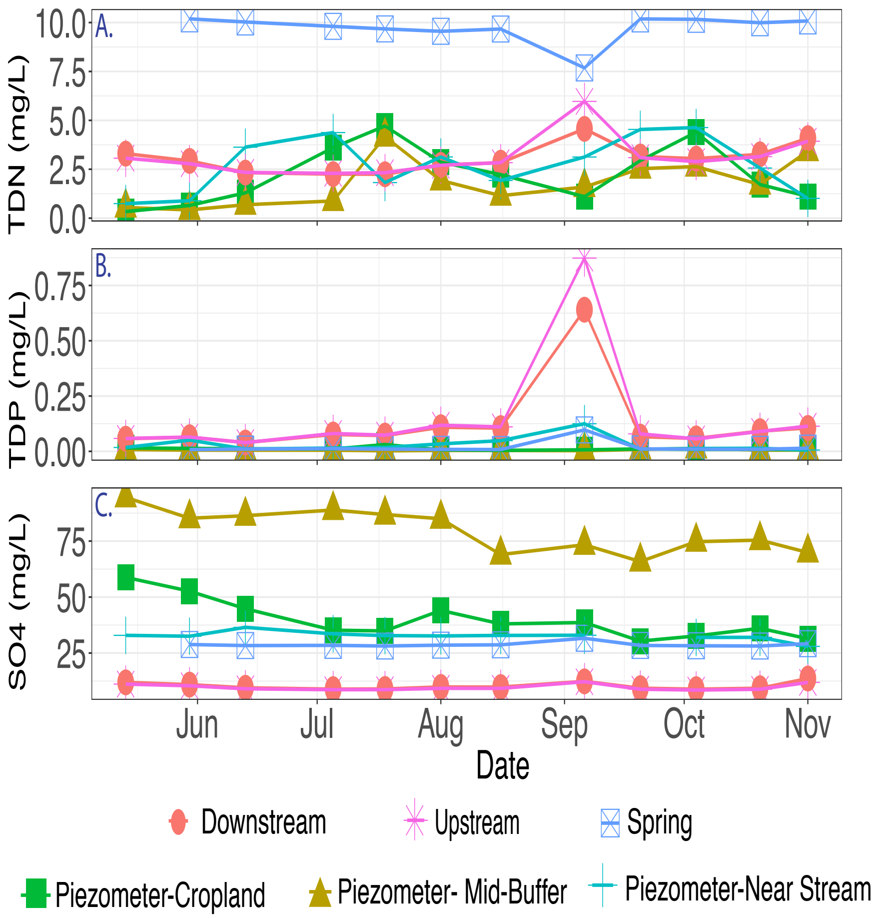

Figure 10 Time series of measured concentrations of A) Total Dissolved Nitrogen (TDN), (B) Total Dissolved Phosphorus (TDP), and (C) Sulfate (SO4) concentrations in mg/L on each sampling date taken from downstream and upstream sites within the mainstem.

B) Intensive Study

The second part of our research focused on objective 5, which was to quantify the extent of interaction between surface water and groundwater within a representative reach that contains a RFBS. A reach in the headwaters of the LACN watershed was selected to quantify this physical interaction and assess the potential interception of groundwater by the vegetation within the riparian buffer. Thus far, analysis of the data collected from the intensive site indicates that the stream is gaining throughout the summer and fall months, suggesting that groundwater flows through the RFBS and discharges into the stream. During sampling in May, however, we classified the direction of surface water-groundwater interaction as "indefinite" (i.e., the difference in discharge between the upstream and downstream stations was within a 5% margin of error that likely represents the uncertainty in our ability to measure discharge using the mid-section method). Measurements of hydraulic head in each piezometer were used to determine the direction of shallow groundwater flow within the riparian zone (i.e., by calculating the hydraulic gradient from the upland portion of the riparian zone to the stream). Using only the measurements for individual sampling dates, we have thus far determined that the hydraulic head gradient measurements are consistent with the stream gaging results insofar as they support a tentative conclusion that this reach is mostly "gaining" through discharge of groundwater through a shallow alluvial aquifer. Additional analysis of the 15-minute water level logger data will be used to test whether this interaction is consistent across a broader set of hydrologic conditions.

Concentrations of constituents measured in the shallow groundwater over the sampling period are shown in Figure 10. Results reveal that water sampled from the piezometer nearest the crop field contained less TDN than the water sampled from the piezometer nearest to the stream, with mid-buffer piezometer most often having the lowest concentration (except for the November sampling date). These results are different from what we hypothesized, as we expected nutrients to be lowest in the piezometer next to the stream (Sabater *et al*., 2003). During the middle of July and August, however, when a large amount of antecedent precipitation may have caused a higher amount of nitrate to run off from the adjacent crop field, water quality seemed to improve in the piezometer closest to the stream. In these instances, higher stream levels may have activated the hyporheic zone and created anaerobic conditions for denitrification. Nevertheless, this hypothesis was tested during the September 6th event when the near-stream piezometer contained the highest TDN compared to the concentrations in the other piezometers. At this time the streamwater itself had the highest TDN concentration—peaking at 5.9 mg/L in the upstream and 4.6 mg/L in the downstream. The spring/tributary that drains into the mainstem had the highest concentration of TDN compared to all sampling sites, where the discharge rate was at its highest at 9.7×10^{-4} cms, but this was still a very small contribution to the stream (about 2%). Moreover, the spring decreased drastically during this event to 7.7 mg/L, where its average concentration was 9.9 mg/L, excluding the concentration measured on September 6th. While the nutrients are the highest in this spring that drains into the mainstem, the influence it has seems to be minimal. Additionally, further upstream from our study site is a large spring that discharges into the mainstem, making up majority of the stream at this location. Therefore, the springs in this region could have a higher concentration in nutrients than the groundwater and the groundwater could be what is gradually diluting the mainstem concentrations.

Results of TDP concentrations showed that groundwater collected from the piezometer directly next to or within the hyporheic zone of the stream had the highest concentrations during summer months and the mid-buffer site usually had the lowest concentration, which is again different from what we expected. The mainstem had the highest concentrations overall with upstream having higher TDP than downstream in most cases. A peak in TDP also occurred during the September 6th event, with upstream containing 0.87 mg/L and downstream containing 0.64 mg/L. The decline may again be due to a dilution effect, since the groundwater collected in the piezometers had drastically lower TDP concentrations than the mainstem. However, given that the TDP concentrations were highest in the piezometer next to the stream, we can infer there was some surface and groundwater exchange during this time.

Measurements of TDN and TDP were used to assess how well a RFBS can mitigate nutrients in groundwater before it discharges into a stream and how this may affect stream water quality. Using a conservative constituent, however, can possibly be used as a tool to determine if the groundwater intersected at each piezometer is from the same source, assuming the concentrations do not change drastically in a linear, subsurface flow. For this analysis, we used only SO_4 concentrations and a pairwise t-test to determine if the water samples taken from the piezometers, upstream and downstream sites, and spring are significantly different from one another. Results from the pairwise t-test showed that sites were significantly different from one another except the upstream and downstream site and the spring and groundwater sampled from the near-spring piezometer. This could infer that the subsurface groundwater flow is not lateral and that the groundwater collected from each of the piezometers originates from different sources. Our next goal is to use the other conservative constituents with a trilinear plot to determine if the samples have their own chemical signatures (Bohlke *et al*., 1995) and determine whether the groundwater collected in the piezometers are mixed with another source, such as emerging deep groundwater and determine if there are corresponding changes with each of the constituents (Jordan *et al*., 1993). Additionally, quantifying the extent of interaction between surface water and groundwater and calculating the net lateral inflow using Darcy's Law and Dupuit's equation will also be performed and compared with the measured nutrients within the stream.

IV) Significance

Defining variables that influence the effectiveness of RFBS within the R&V can help organizations locate sites that will best improve stream water quality. Our results suggest that the hydrological characteristics are important in understanding how well RFBS mitigate nutrients from groundwater before it is discharged into receiving waters. We found in many instances that tributaries and springs influenced stream water quality more than the presence of RFBS or forested areas within the watersheds and the models used to estimate nutrient fluxes within the R&V can be more reliable if they use actual flow data. However, there were instances when both models were better at predicting concentrations than the other and were independent from the subwatershed and constituent. Therefore, this further supports the challenge of understanding the hydrological systems that control nutrient concentrations in streams and RFBS function. Our results did not support the idea that RFBS significantly reduce TDN and TDP in watersheds within the R&V, but there was some support with the results found at LACS where majority of the mainstem is made up of lateral groundwater. More analyses will be performed to investigate how much TDN and TDP each stream reach should have received based on the surrounding crop type in each watershed. Knowing the specific crops planted using Cropscape data layer and how much fertilizer is typically applied to these crops using University of Maryland Extension website (https://extension.umd.edu), we can estimate how much nutrients are typically lost in groundwater and if nutrient concentrations in the adjacent streams were lower than expected because of the presence of a RFBS. This will further test if RFBS are reducing nutrients at these sites. Analyses will also be performed to determine if any correlation exists between karst and other geological features that may be affecting RFBS function.

V) References

Bohlke, J. K., and J. M. Denver (1995). Combined use of groundwater dating, chemical, and isotopic analyses to resolve the history and fate of nitrate contamination in 2 agricultural watersheds, atlantic coastal-plain, Maryland (Paper 95WR01584). *Water Resources Research, 31*, p. 2319-2339.

Boynton, W. R., Kemp, W. M., & Keefe, C. W. (1982). A comparative analysis of nutrients and other factors influencing estuarine phytoplankton production. 69-90.

Clement, J. C., Holmes, R. M., Peterson, B. J., & Pinay, G. (2003). Isotopic investigation of denitrification in a riparian ecosystem in western France. *Journal of Applied Ecology*, *40,* 6, 1035-1048.

Department of Natural Resources (DNR) (2014). The Maryland Conservation Reserve Enhancement Program: 2013 Annual Report.

Fisher, T. R., Peele, E. R., Ammerman, J. W., & Harding, L. W. (1992). Nutrient limitation of phytoplankton in Chesapeake Bay. *Marine Ecology Progress Series, 82*, 1, 51-63.

Gallegos, C. L., Jordan, T. E., & Correll, D. L. (1992). Event-scale response of phytoplankton to watershed inputs in a subestuary: Timing, magnitude, and location of blooms. *Limnology and Oceanography, 37*, 4, 813-828.

Gold, A. J., P. A. Jacinthe, P. M. Groffman, W. R. Wright, and R. H. Puffer (1998). Patchiness in groundwater nitrate removal in a riparian forest. *Journal of Environmental Quality, 27*, 1, 146.

Herbst, David (2017). Email interview.

Hill AR. (1996). Nitrate removal in stream riparian zones. *Journal of Environment Quality*. 25, 4, 743.

Homer, C.G., Dewitz, J. A., Yang, L., Jin, S., Danielson, P., Xian, G., Coulston, J., Herold, N. D., Wickham, J. D., and Megown, K., (2015). Completion of the 2011 National Land Cover Database for the conterminous United States- Representing a decade of l and cover change information. Photogrammertric Engineering and Remote Sensing, v. 81, no. 5, p. 345-354.

Jacobs, T. C., & Gilliam, J. W. (1985). Riparian Losses of Nitrate from Agricultural Drainage Waters1. *Journal of Environment Quality*, 14, 4, 472.

Jordan, T. E., Correll, D. L., Miklas, J., & Weller, D. E. (1991). Nutrients and chlorophyll at the interface of a watershed and an estuary. *Limnology and Oceanography*, 36, 2, 251-267.

Jordan, T. E., Correll, D. L., & Weller, D. E. (1997). Relating nutrient discharges from watersheds to land use and streamflow variability. *Water Resources Research*, 33, 11, 2579-2590.

Jordan, T. E., Correll, D. L., & Weller, D. E. (1993). Nutrient Interception by a Riparian Forest Receiving Inputs from Adjacent Cropland. *Journal of Environmental Quality*, 22, 3, 467.

Lowrance, R. L. S. Altier, J. D., Newbold, R. R. Schnabel, P. M. Groffman, J. M. Denver, D. L., Correll, J. W. Gilliam, J. L., Robinson, R. B. Brinsfield, K. W. Staver, W. Lucas, and A. H. Todd (1997). Water quality functions of riparian forest buffers in Chesapeake Bay watersheds: *Environmental Management, 21,* 5, 687-712.

Malone, T. C., Kemp, W. M., Ducklow, H. W., Boynton, W. R., Tuttle, J. H., & Jonas, R. B. (1986). Lateral variation in the production and fate of phytoplankton in a partially stratified estuary. *Marine Ecology Progress Series, 32*, 149-160.

Maryland Department of Natural Resources (MDDNR) (n.d.). Wetlands and Forest Management. Retrieved May 20, 2018 from http://dnr.maryland.gov/forests/Pages/programapps/rfbrestoration.aspx.

Maryland Department of Transportation (MDOT) State Highway Administration (SHA) (2017). Maryland Statewide Salt Management Plan. Retrieved May 20, 2018 from http://roads.maryland.gov/oom/statewide_salt_management_plan.pdf.

Messer, T. L., Burchell, M. R., Grabow, G. L., & Osmond, D. L. (2012). Groundwater nitrate reductions within upstream and downstream sections of a riparian buffer. *Ecological Engineering, 47*, 2, 297-307.

Sabater, S. Butturini, A., Clement, J. C., Burt, T., Dowrick, D., Hefting, M., Matre, V., … Sabater, F. (2003). Nitrogen Removal by Riparian Buffers along a European Climatic Gradient: Patterns and Factors of Variation. *Ecosystems*, *6*, 1, 20-30.

Schoonover, J. E., and K. W. J. Williard (2003). Ground water nitrate reduction in giant cane and forest riparian buffer zones. *Journal of the American Water Resources Association, 39*, p. 347-354.

Seneca Valley Trout Unlimited (SVTU) (n.d.). Seneca Valley Trout Unlimited. Retrieved April 18, 2018 from http://www.senecavalleytu.org/SubPages/BeaverCreek.html.

Snyder, N. J., Mostaghimi, S., Berry, D. F., Reneau, R. B., Hong, S., McClellan, P. W., & Smith, E. P. (1998). Impact of riparian forest buffers on agricultural nonpoint source pollution. *Jawra Journal of the American Water Resources Association, 34,* 2, 385-395.

Soil Survey Staff, Natural Resources Conservation Service, United States Department of Agriculture. Web Soil Survey. Available online at the following link: https://websoilsurvey.sc.egov.usda.gov/.Accessed [Oct 1, 2017].

Solomon, D. , Lehmann, J. , Kinyangi, J. , Pell, A. , Theis, J. , Riha, S. , Ngoze, S. , Amelung, W. , Preez, C. , Machado, S. , Ellert, B. and Janzen, H. (2009). Anthropogenic and climate influences on biogeochemical dynamics and molecular-level speciation of soil sulfur. *Ecological Applications, 19*, 4, 989-1002.

Sutton, A. J., Fisher, T. R., & Gustafson, A. B. (2010). Effects of Restored Stream Buffers on Water Quality in Non-tidal Streams in the Choptank River Basin. *Water, Air, and Soil Pollution an International Journal of Environmental Pollution, 208,* 101-118.

USDA National Agricultural Statistics Service Cropland Data Layer. {2016}. Published crop-specific data layer [Online]. Available at https://nassgeodata.gmu.edu/CropScape/ (accessed {April 2018}; verified {2018}). USDA-NASS, Washington, DC.

United States Environmental Protection Agency (USEPA), Region III (2015). Little Antietam Creek Watershed Assessment Report. Retrieved May 20, 2018 from https://www.epa.gov/sites/production/files/2015-07/documents/littleantietamcreekwatershedassessmentreport_0.pdf.

Weller, D. E., M. E. Baker, and T. E. Jordan (2011). Effects of riparian buffers on nitrate concentrations in watershed discharges: new models and management implications. *Ecological Applications*, *21*, 5, 1679-1695.

Winter, T.C., J. W. Harvey, O. L. Frank, and W. M. Alley (1998). Ground Water and Surface Water. *A Single Resource*. Circular 1139.

VI) Publications and Presentations

Siemek, S., & Eshleman, K. (2017, June). Assessing riparian hydrologic pathways as controls on forested buffer function in four sub-watersheds in western Maryland. Poster Presentation. Gordon Research Conference: Catchment Science, Lewiston, ME.

Siemek, S., & Eshleman, K. (2017, Dec.). Assessing riparian hydrologic pathways as controls on forested buffer function in four sub-watersheds in western Maryland. Oral presentation, Maryland Water Monitoring Council Conference, Linthicum, MD.

Two manuscripts are in progress based on the material presented in 2017 at the Gordon Research Conference and the 2017 Maryland Water Monitoring Council Conference.

VII) Students supported

Ph.D.

The project provided the primary research funding for Stephanie Siemek, a Ph.D. student in the MEES program who was advised by the project PI.

Impact of the "308 Reports" on Water Resources Planning and Development in the United States and Implications of the Results for the Future

Basic Information

Title:	Impact of the "308 Reports" on Water Resources Planning and Development in the United States and Implications of the Results for the Future
Project Number:	2016MD347S
USGS Grant Number:	
Sponsoring Agency:	Army Corps of Engineers
Start Date:	2/7/2016
End Date:	9/6/2017
Funding Source:	104S
Congressional District:	MD-005
Research Category:	Social Sciences
Focus Categories:	Law, Institutions, and Policy, None, None
Descriptors:	None
Principal Investigators:	Kaye Lorraine Brubaker

Publications

There are no publications.

Jeffrey Brideau, Ph.D.

June 1, 2017

Project Progress Summary

Maryland Water Resources Research Center

Below, is a brief summary of the progress made on the project *Impact of the "308 Reports" on Water Resources Planning and Development in the United States and Implications of these Results for the Future*, funded by the National Institutes of Water Resources (NIWR) through a grant administered by the United States Geological Survey (Grant/Cooperative Agreement Number G16AP00019).

In January 1927, the U.S. Congress, speaking through the Rivers and Harbors Act (PL 70-560), instructed the U.S. Army Corps of Engineers (USACE) to prepare a nationwide series of river surveys to determine the feasibility of developing hydroelectric power in combination with navigation, irrigation, and flood control measures. Collectively known as the "308 Program" – named after House Document 308, 69th Congress, 1st Session, which defined the surveys' scope and intent – this program marked the first national, basin-wide, multipurpose water resources planning program in the United States.

The stated objective of this research project is:

> "to explore the linkages between the production of large-scale water resources planning studies by a federal agency, and the material development of water resources at the federal, state, and local levels. Through the analysis of the set of reports, participant motivations, as well as contemporary economic and political events, key lessons will be sought with applications for the development of 21st century water resources planning in the United States."

To achieve these objectives, the co-PI – Dr. Jeffrey Brideau – developed an archival research agenda, identified and reviewed the secondary literature, and proposed a set of project outputs. Early in the project, Dr. Brideau identified a set of archival repositories and specific record groups for the collection of data related to specific case studies. Accordingly, he travelled to archives in Augusta, Athens, and Atlanta, Georgia to examine and capture records related to the Savannah District's 308 report; as well as records from the Office of the Chief of Engineers (RG 77) at the National Archives and Records Administration facility in College Park, Maryland. In sum, Dr. Brideau collected over 10,000 research documents, which were copied, indexed, scanned with optical character recognition, and annotated. Additionally, the 308 surveys have been located, organized, and made publically available on the website of USACE's Institute for Water Resources' website [http://www.iwr.usace.army.mil/Library/IWR-Library/308-Reports-Series/].

Over the past year, Dr. Brideau reviewed this abundance of the archival and secondary material. Last autumn, at the outset of the project's second phase, he presented his preliminary findings to a large group of IWR and University of Maryland scholars in a presentation entitled: *Designing Rivers, Redesigning Institutions: The U.S. Army Corps of Engineers' 308 Reports*. Incorporating the feedback from that presentation and subsequent discussions, Dr. Brideau developed a historical narrative that includes a set of historical and strategic policy lessons to be incorporated into a set of reports, papers, and a presentation. In May of 2017, he submitted a report that delineated the history of the 308 program, including the Savannah River case study, and proposed seven historical lessons as well as eight lessons for decision-makers to consider in the construction of a national-scale water resources strategy. This report was well received within IWR and its reception prompted a reevaluation of the proposed project outputs.

First, during the summer of 2017, the co-PI will produce a modified report for publication by IWR that is composed of a set of historical vignettes that advance lessons for constructing a national water resources strategy. This report will be complemented by a presentation addressed to USACE leadership and other water resources decision makers. Second, the co-PI has engaged the editor-in-chief of the *Journal of Water Policy* about the submission of a peer-reviewed article that delineates the findings of the aforementioned report. They are corresponding about a timeframe for submission, review, and revision; and the co-PI plans to have this paper submitted by Autumn 2017. Third, the Co-PI has proposed a later submission of a second peer-reviewed article to the journal *Environmental History* focused on the research's historiographical interventions – in particular, the institutional transformation of USACE from a dam adverse agency to dam enthusiasts within a national big-dam consensus. Finally, in terms of proposed publications, the PI and co-PI have discussed placing a short article in a significant engineering magazine (e.g. *Civil Engineering* or *The Military Engineer*) to reach a wider audience and publicize ongoing research. Drafts of these publications, in various stages of completion and revision, can be made available upon request.

In terms of data management and dissemination, the co-PI is working with the USACE Office of History to digitally retain and offer wider access to the substantial volume of research materials collected. Dr. Brideau has also worked with the USACE Office of History and U.S. Army's Center for Military History to establish an oral history project at IWR. These oral histories are designed to capture individual stories related to water resources planning and development as well as institutional dynamics at IWR. To date, Dr. Brideau has conducted, recorded, and assembled seven oral history interviews with senior and retired staff at IWR as well as past recipients of the Maass-White fellowship. Several more interviews are planned and scheduled over the upcoming months – with the goal of 15 interviews completed by the end of 2017. Once there is a critical mass of interviews, they will be transcribed, edited, and published by IWR. The oral history component of this will complement a written history of IWR awaiting publication, capture institutional memory at the Institute, and offer a variety of perspectives on

IWR's evolution, the current state of water resources planning and development, and ideas for its future.

Additional information on the project's status, ongoing research endeavors, citations, submitted reports or anticipated publications and other outputs can be provided by contacting the co-PI at: jbrideau@umd.edu.

Can Carbon Amendments Improve Wetland Restoration and Jump-Start Microbial Activity?

Basic Information

Title:	Can Carbon Amendments Improve Wetland Restoration and Jump-Start Microbial Activity?
Project Number:	2017MD340B
Start Date:	3/1/2017
End Date:	2/28/2018
Funding Source:	104B
Congressional District:	MD-005
Research Category:	Biological Sciences
Focus Categories:	Wetlands, Ecology, Nutrients
Descriptors:	None
Principal Investigators:	Stephanie Ann Yarwood, Andrew Baldwin

Publications

There are no publications.

Status Report

Can Carbon Amendments Improve Wetland Restoration and Jump-Start Microbial Activity?

Prepared for: Maryland Water Resources Research Center Project Number: 2017MD340B

Project duration: March 1, 2017 - February 28, 2019

Principal Investigator: Stephanie A. Yarwood

Department of Environmental Science and Technology
University of Maryland, College Park, MD 20742

syarwood@umd.edu 301-405-1345

Co-PI: Andrew H. Baldwin

Prepared by: A.H. Baldwin, S.A. Yarwood, and

Brian Scott (graduate student)

Submitted: May 31, 2018

Project Goals, Methods, and Research Accomplishments

Objectives

Objective 1: Identification of organic matter (OM) amendments (e.g. compost) that promote desired wetland functions (e.g. iron reduction).

Objective 2. Determine the loading rate of OM amendments that best promotes hydric soil conditions.

Objective 3: Improve our understanding of the microorganisms responsible for decomposition and the fate of OM in restored wetlands.

Methods

This experiment is being conducted in two phases. Phase I: determine the fate of OM amendments and the type of microbial processes they promote (e.g. denitrification, iron reduction and/or methanogenesis). Phase II: determine the bacteria that are stimulated by the OM amendments, in particular, whether or not iron reducing bacteria are stimulated.

The first mesocosm experiment was initiated in May 2017. We collected unamended soil samples from a wetland restoration site near Clinton, Maryland. Soil samples were sieved to 2mm and composited. This experimented evaluated the use of 5 amendments at 3 loading rates. Amendments were BLOOM™ (a class "A" biosolid from DC Water), LeafGro (composted yard waste from Montgomery county MD), manure (horse manure), mulch (hardwood mulch) and hay. Loading rates were based on the Maryland Department of Environment (MDE) required loading rate of 113.4 m^3/ha. Amendment levels were 1x, 3x and 6x the MDE required rate. The bulk density of composited soil, each OM amendment, and the blended material were measured to covert the loading rates to a weight/weight ratio.

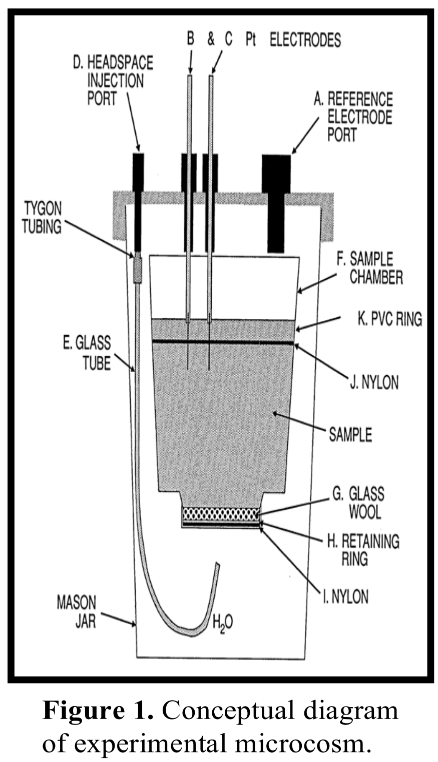

Figure 1. Conceptual diagram of experimental microcosm.

Per our proposal, we had planned to set up mesocosms using 1000-mL Nalgene™ Straight-Sided Wide-Mouth Jars (Figure 1). However, after running preliminary experiments we determined that the Nalgene jars were permeable to oxygen and this adversely affected our ability to monitor iron reduction. Therefore, we modified our experimental design to use glass wide mouth ball jars. Rather than use platinum electrodes, we monitored the development of reducing conditions with iron and manganese oxide coupons. The metal oxides were sequentially removed (manganese then iron) from the coupons as reducing conditions developed.

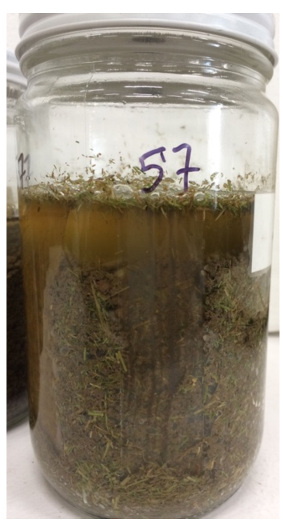

Figure 2. Mesocosm jar with coupons

The jar headspace was monitored for the evolution of carbon dioxide, methane and nitrous oxide gasses.

After the soil, water and amendments were added to the mesocosms, the jars were sealed and the headspace was purged with nitrogen gas. A second set of mesocosms were prepared with an air headspace to verify that the presence of oxygen did not alter the soil biochemistry. A third set of mesocosms were amended with ferrihydrite or goethite to determine if either of these would contribute to iron reduction.

Figure 3. Mesocosm setup crew.

All mesocosms were monitored for the following parameters at the beginning and end of the experiment: Total organic matter (by loss on ignition), Total carbon and total nitrogen, microbial organic carbon and nitrogen (by fumigation), and extractable nitrate, ammonia and total phosphorous. Headspace gas samples were collected periodically depending on the gas production rate.

The Phase II mesocosm study will be conducted in the Fall and Winter of 2018. Originally, we were planning a Stable Isotope Probe DNA labelling experiment using ^{18}O-H_2O. However, based on our experimental results to date, we will be modifying this experiment to use ^{13}C-labeled substrates. This will have several advantages over ^{18}O-H_2O. First, ^{13}C-labeled substrates are significantly less expensive, and our experimental size can be scaled up to match our mesocosms in Phase I. Second, our initial experiments have suggested that the driver of anaerobic processes, particularly iron reduction, is substrate driven and ^{13}C-labeling allows us to track the fate of the substrates as the stable isotope ^{13}C is incorporated into cell DNA, and also as $^{13}CO_2$ and $^{13}CH_4$ is produced. Other elements of the experiential design will be as described in our proposal.

Research synergy

Our original proposal was supported by the Maryland State Highway Administration (SHA). SHA gave us permission to use soils from their planned mitigation site near Goldsboro, MD (Smith Farm). However, MDE has also been able to supply funding for a companion research project in close alignment with this MWRRC funded project. As a result, we are currently conducting a second Phase I mesocosm experiment, which we will designate Phase Ib, using soils from the Smith Farm site. The Smith Farm soils are sands, as compared to loam soil from the Clinton site. These two sites will allow us to compare the results using similar amendments on differing soil types, enhancing the applicability of our results. The SHA is also funding a companion field study, so we will be able to directly compare our mesocosm results to field observations. The field study is currently scheduled to take place in the summer of 2019.

Research accomplishments

Results from the Phase Ia mesocosm study have been helpful in guiding our modifications for the Phase II study. The data provided here are the main findings that have informed Phase II planning. Some results from the Phase Ia study (using sandy loam soil) are best evaluated in comparison to our Phase Ib study (using loamy sand soil). Those results will be presented after completion of Phase Ib.

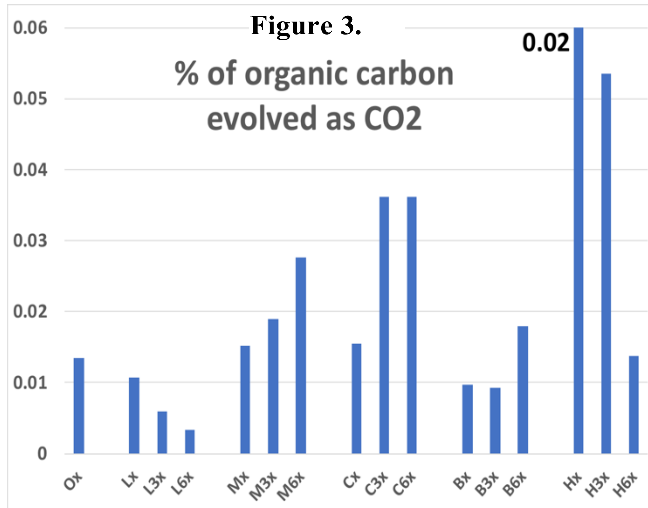

The amount of gas produced in our mesocosms represented only a small fraction of the total amount of organic carbon in the system (Figure 3). A smaller fraction of carbon evolved as methane gas. The amount of carbon dioxide was generally less than 0.04% , suggesting there is a very small labile fraction of the total organic carbon which is responsible for the observed biogenic activity. LeafGro (L) is very well composted and contains little labile carbon. Adding LeafGro displaced soil in the mesocosm so the amount of labile carbon, which was already present in the soil, went down. In general, the least composted amendments produced the most biogeneic gas.

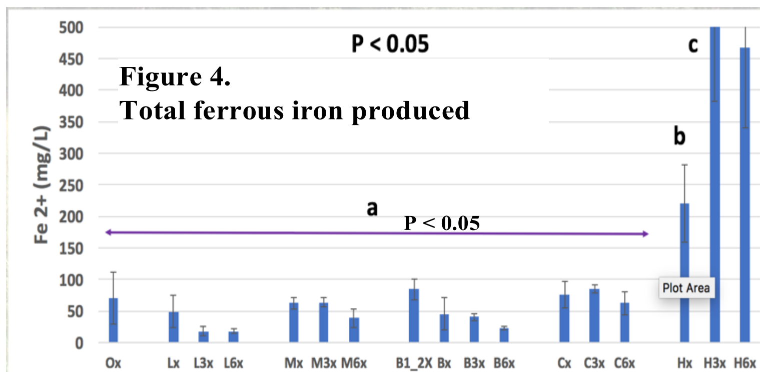

We observed a similar pattern in the amount of ferrous iron produced in the system, which also appears to be a function of the amount of labile (fermentable) carbon. The undigested hay amendment had significantly higher rates of both carbon dioxide (Figure 3) and ferrous iron production (Figure 4).

Studies have shown that the form of iron in soils can influence the microbial activity. Soils that are higher in amorphous iron (ferrihydrite) can support iron reduction whereas soils with hematite and goethite may not (Lovley and Phillips 1986). Therefore, we examined the amount, and form, of iron present in the soil from our two sites. While there is not a large difference in the amount of organic carbon from each soil, the amount of extractable iron in the Smith Farm soils is much lower (Table 1).

Table 1. Extractable Iron and Percent Organic Carbon

mg Fe/ g soil (dry weight)	Acetate	Dithionite	Oxalate	Percent Organic Carbon
Phase Ia Clinton (sandy loam)	0.15	2.24	2.51	1.76
Phase Ib Smith Farm (loamy sand)	0.03	0.29	0.79	1.15

Lovley, Derek R., and Elizabeth JP Phillips. 1986. "Organic Matter Mineralization with Reduction of Ferric Iron in Anaerobic Sediments." *Applied and Environmental Microbiology* 51 (4): 683–689.

In the Phase Ia mesocosm experiment we prepared a set of mesocosms using ferrihydrite as an amendment but there was no increase in ferrous oxide production. Prior starting our Phase Ib experiment, we performed a small study using soil from the Smith Farm site. In this mesocosm we amended with ferrihydrite (only), hay (only) and ferrihydrite + hay. The addition of ferrihydrite did not stimulate ferrous iron production over the unamended soil (Figure 5). This suggests that these soils have limited labile

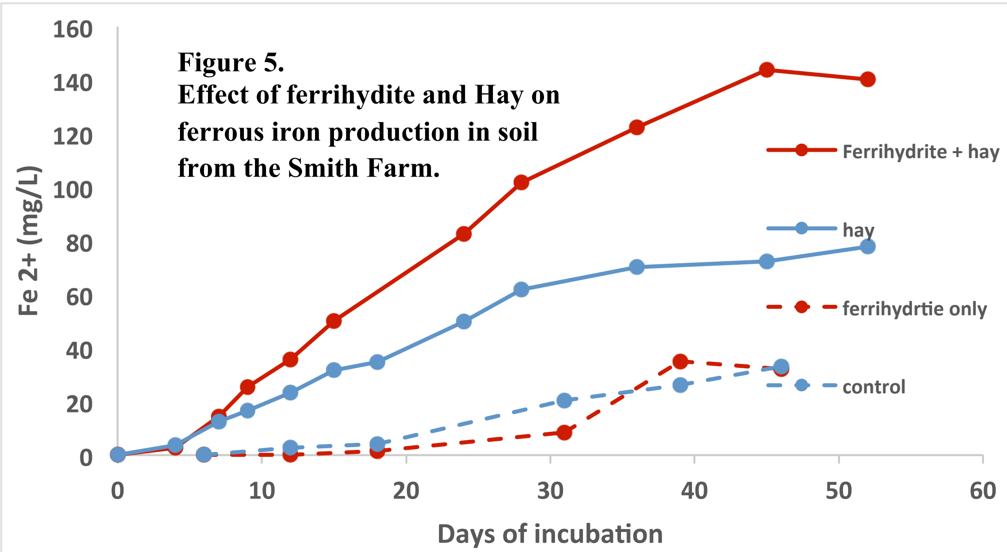

Figure 5.
Effect of ferrihydite and Hay on ferrous iron production in soil from the Smith Farm.

carbon to stimulate iron reduction. Hay significantly increased iron production and when added with ferrihydrite, produced the largest increase in ferrous iron. Thus, even though there appears to be a limitation in the amount of easily reducible (labile) iron oxide, it is the availability of a labile (fermentable) carbon substrate the controls microbial activity.

Since it appears that a source of labile carbon is the driver in our system, we theorized that the soluble (leachable) fraction of the hay contained most of the labile fraction. However, this does not appear to be the case. In an experiment comparing leached hay and leachate, the leached hay stimulated more iron reduction than leachate and was similar to un-leached hay (Figure 6).

This may explain a peculiar finding from our Phase Ia experiments. I was apparent that the amount of carbon dioxide decreased as the hay loading rate increase (Figure 3). This is not likely due to reduction in labile carbon as was the case with LeafGro. A more likely explanation is from OM amendment rafting. The hay produced such high levels of biogas in the early part of the

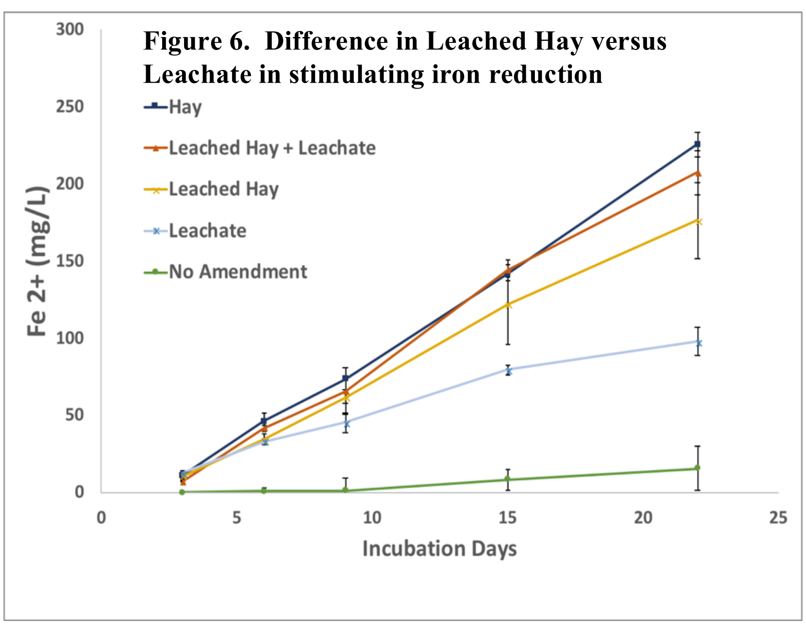

Figure 6. Difference in Leached Hay versus Leachate in stimulating iron reduction

incubation that the gas bubbles caused effervescing, disturbing the soil so that the Hay rafted to the surface. This phenomena was not apparent until we began observations on our Phase Ib experiment. The sandy soils used for Phase Ib are less cohesive and OM amendment rafting much more pronounced (hay, mulch and LeafGro are all exhibiting rafting at high dose levels). As a result, the hay in the 3x and 6x mesocosms have rafted to the surface and are not in contact with the soil matrix (Figure 7). Since the labile carbon in the hay is associated more with the solid fraction, rafting leads to less microbial activity. For example, in the mesocosms in Figure 7, M6x-2 is producing significantly more gas and ferrous iron than H6x-3 (Data not shown).

Figure 7. Rafting in high dose Hay mesocosms.

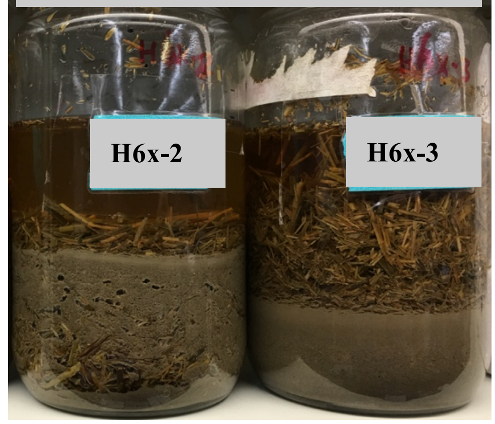

As a consequence of these findings, we are planning to modify Phase II to include ^{13}C-labeled substrates that are representative of the solid fraction of hay (e.g. lignin and cellulose). We will also select two types of soils, one that is high in amorphous iron and one that is low in amorphous iron similar to those we have used in Phase I.

Publications and Presentations

The first planned presentation of our findings will be at the SSSA meeting in San Diego, January 2019. We are also planning to submit two publication following completion of the experiments. One manuscript will focus on the effect of OM amendments with different soil types and the second will focus on the differences in microbial populations as a consequence of soil and substrate types.

Students Supported: Undergraduate

The project has made possible the support of Donald DeAlwis who has been very active in all aspects of the work. Additionally, 5 undergraduate students working in the PIs' labs have participated in the project and discussed the project during presentations given by the graduate student during lab group meetings.

M.S. No M.S. students were directly supported in this work; however, they also participated in lab group meetings and discussions.

PhD The project provided the primary research funding for PhD student Brian Scott.

Listening to Rivers: Seismic and Hydraulic Monitoring to Determine River Turbulence and Erosive Power

Basic Information

Title:	Listening to Rivers: Seismic and Hydraulic Monitoring to Determine River Turbulence and Erosive Power
Project Number:	2017MD341B
Start Date:	3/1/2017
End Date:	4/30/2018
Funding Source:	104B
Congressional District:	MD-005
Research Category:	Climate and Hydrologic Processes
Focus Categories:	Geomorphological Processes, Surface Water, Floods
Descriptors:	None
Principal Investigators:	Karen Prestegaard, Vedran Lekic

Publication

1. Goodling, P. J., Lekic, V., and Prestegaard, K.: 2018, Seismic signature of turbulence during the 2017 Oroville Dam spillway erosion crisis, Earth Surf. Dynamics. https://doi.org/10.5194/esurf-2017-71

Completion Report

Listening to Rivers: Seismic and Hydraulic Monitoring to Determine River Turbulence and Erosive Power

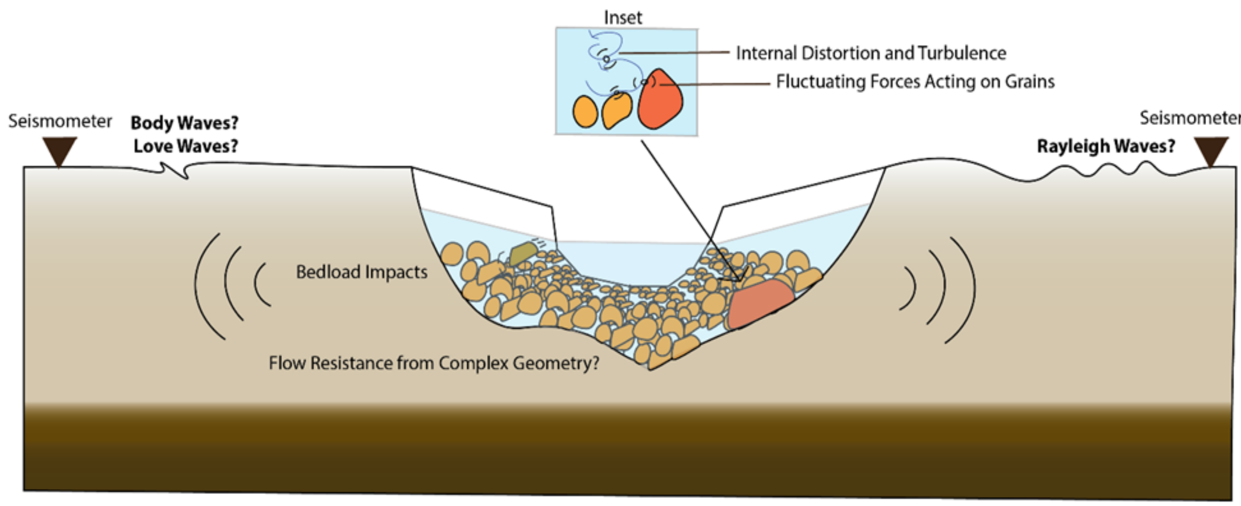

Prepared for: Maryland Water Resources Center

Project Number: 2017MD341B

Project Duration: 1 Yr

Principal Investigators:
Karen Prestegaard
Vedran Lekic
Department of Geology
University of Maryland
College Park, MD 20742
kpresto@umd.edu 301-405-6982
ved@umd.edu 301-405-4086

Prepared by: K. Prestegaard, V. Lekic, P. Goodling (graduate student)

Project goals, methods, and research accomplishments

Objectives:

1. To characterize channel morphology (width, depth, gradient, grain size distributions) along bedrock and alluvial river reaches.
2. To monitor stream hydraulics (discharge, velocity, gradient) with high temporal resolution during high flow events to
3. To use a seismograph array along river reaches to record seismic noise for selected flow events.
4. To develop procedures to separate seismic noise caused by streamflow and sediment transport from other sources of seismic noise.
5. To use compare field observations of turbulent seismic noise with existing models of roughness-generated turbulence in rivers. .
6. To develop a cross-disciplinary field research experience for students in geomorphology and seismology courses.

Study Sites and Methods:

Field work was conducted on the Northwest Branch of the Anacostia River, which is a stream in a suburbanized watershed located north of Washington, DC (fig. 1a). The initial selected study reach is a boulder-bed site located above the Atlantic Fall line, which separates the Piedmont and Coastal Plain provinces in Atlantic Slope basins. The reach is straight, contains two pools and two riffles and discharge is assumed to be constant over the reach (no tributaries enter the reach). Gauges are located upstream and downstream of the study reach (fig.1b); data from these gauges were used to construct rating curves for the gauges installed in the study reach.

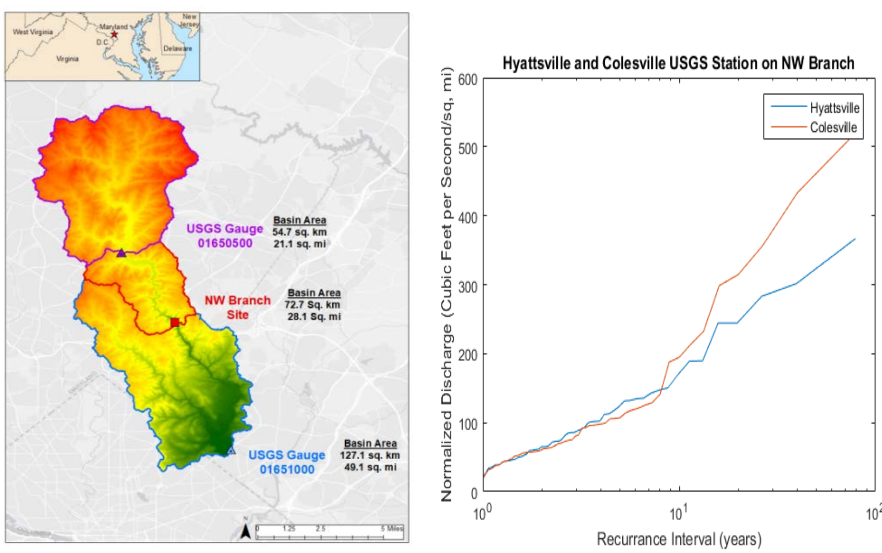

Fig. 1: Left image: map of the NW Branch Anacostia River, showing study site and gauge locations. Right image: normalized flood frequency curves indicating the similarity of unit discharge for the two gauges for floods with R.I of 10 years or less.

Measurements of channel morphology and hydraulics: Channel morphology was measured by surveying ten channel cross-sections spaced at 10-meter intervals along the river reach. Grain size data were collected using the Wolman pebble count method at cross section locations and analyzed to obtain median, D_{50}, and D_{84} (standard deviation above the mean) grain size data. Stream gauges were installed at three locations along the reach, and their elevations were surveyed to the same benchmark as the channel cross sections. The stream gauges recorded water levels at 5 minute intervals over the study period. These data were converted to water surface elevation data and used to determine the dynamic response of water surface gradients during storms (gradient = Δ elevation/distance). The combination of gauge and survey data was used to monitor river cross sectional area (A), width (W), average depth (d), and relative particle submergence (d/D_{84}) at each cross section during storm events. Correlation of gauge height measured in the reach with unit discharge obtained from USGS gauges provided information to construct gauge height-discharge rating curves for the study reach. Instantaneous discharge (Q), data for the reach were used to calculate velocity, stream power (ρgQS), shear velocity ($u^* = (gdS)^{0.5}$), and other hydraulic parameters. A schematic diagram of the reach with monitoring equipment is shown in fig. 2a. Surveyed channel cross sections are shown in fig. 2b.

Seismic monitoring network: Seismic data was collected from six Fairfield Zland three-component seismic nodes that were set to record data at 250 Hz sampling frequency. The seismic nodes were deployed in 15 cm deep holes. Nodes were leveled with a bubble level, and were oriented towards true north, so that the horizontal channels record north-south and east-west ground motions. Six nodes were placed in the cross-shaped array shown in (fig. 2a), which was designed to characterize the along-channel variability of seismic energy, provide an opportunity to investigate signal attenuation with distance from the channel, and evaluate the interference of noise from other sources such as wind, trees, rain, and traffic.

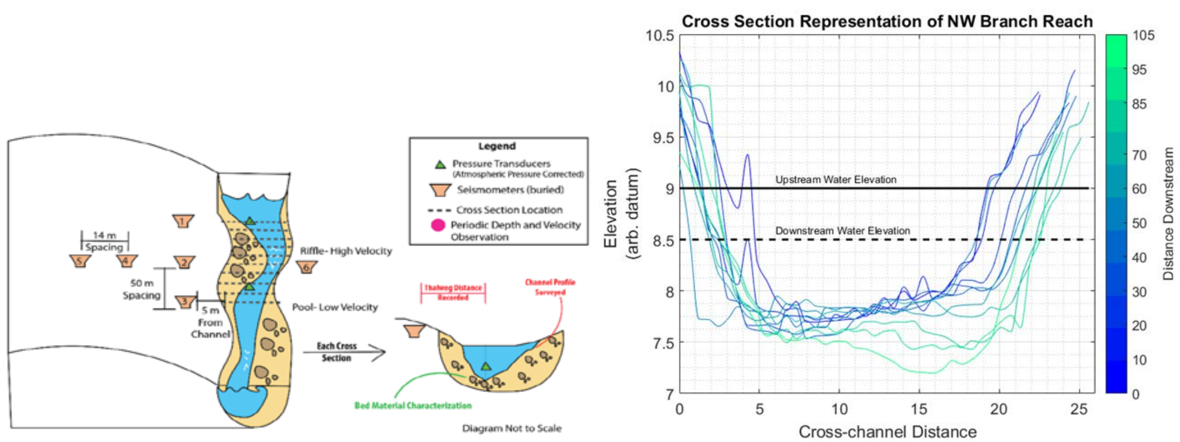

Fig. 2: Left image: Schematic diagram illustrating the location of channel cross section (dashed lines), stream gauges (triangles), and buried seismometers (brown symbols) in the study reach. Right image: Channel cross sections color-coded by distance downstream and the base flow water elevation at the time of the initial survey.

Seismic Data Analysis:

The three-component seismic data was analyzed for its frequency content by performing a discrete Fourier Transform of the data, which yields complex Fourier coefficients for the data as a function of frequency. For time-varying signal $g(t)$, sampled at time intervals of Δt, the discrete Fourier transform of the data $G(\omega_j)$is:

$$G(\omega_j) = \frac{1}{N}\sum_{k=0}^{N-1} g_k e^{-i\omega k\Delta t}$$

where ω_j is the angular frequency, k is the sampling interval in units of time such that $t = k\Delta t$, and N is the total number of samples such that the total time of the signal is $T = N\Delta$t. The frequency interval between successive $\omega_j's$ discrete Fourier coefficients is $\Delta v \ = \frac{1}{T}$. One property of the discrete Fourier transform is a tradeoff between frequency resolution and time resolution of the signal. Another is the assumption that the signal is non-time varying. A third is the Fourier coefficients are only interpretable up to the Nyquist frequency of $\frac{1}{2\Delta t}$.

The power spectral density from discrete Fourier coefficients will be used to evaluate the seismic energy excited by river processes. The power spectral density S_{xx} is the square of the discrete Fourier Transform coefficients, and represents the energy per unit frequency. Because the coefficients are complex numbers, the power spectral density is calculated as:

$$S_{xx}(\omega_j) = |G(\omega_j)|^2 = G(\omega_j) \times G(\omega_j)^*,$$

where the asterisk denotes complex conjugation. To limit the influence of short-lived and high power noise in the environment that can result from human activity or wildlife, the average power in a 5 minute time interval will be determined using windowing methods applied in Goodling, Lekic, and Prestegaard (2018).

Analysis of flood event data:

Thirteen flood events of varying magnitude and duration were monitored in the summer and fall of 2017. For each flood event, geomorphic, hydraulic, and seismic data are analyzed. Examples of analyzed hydraulic and seismic data obtained during a fall, 2017 storm event are presented in fig. 3. This figure illustrates the hydrograph (as river stage or depth), several hydraulic variables (gradient, shear velocity, u*), precipitation rate, wind gusts, and seismic noise. The objective of this research is to determine whether seismic noise can be used to evaluate energy dissipation due to turbulence. Therefore, the noise created by rain, wind, trees, and traffic must be removed from the seismic signal before comparison with hydraulic data.

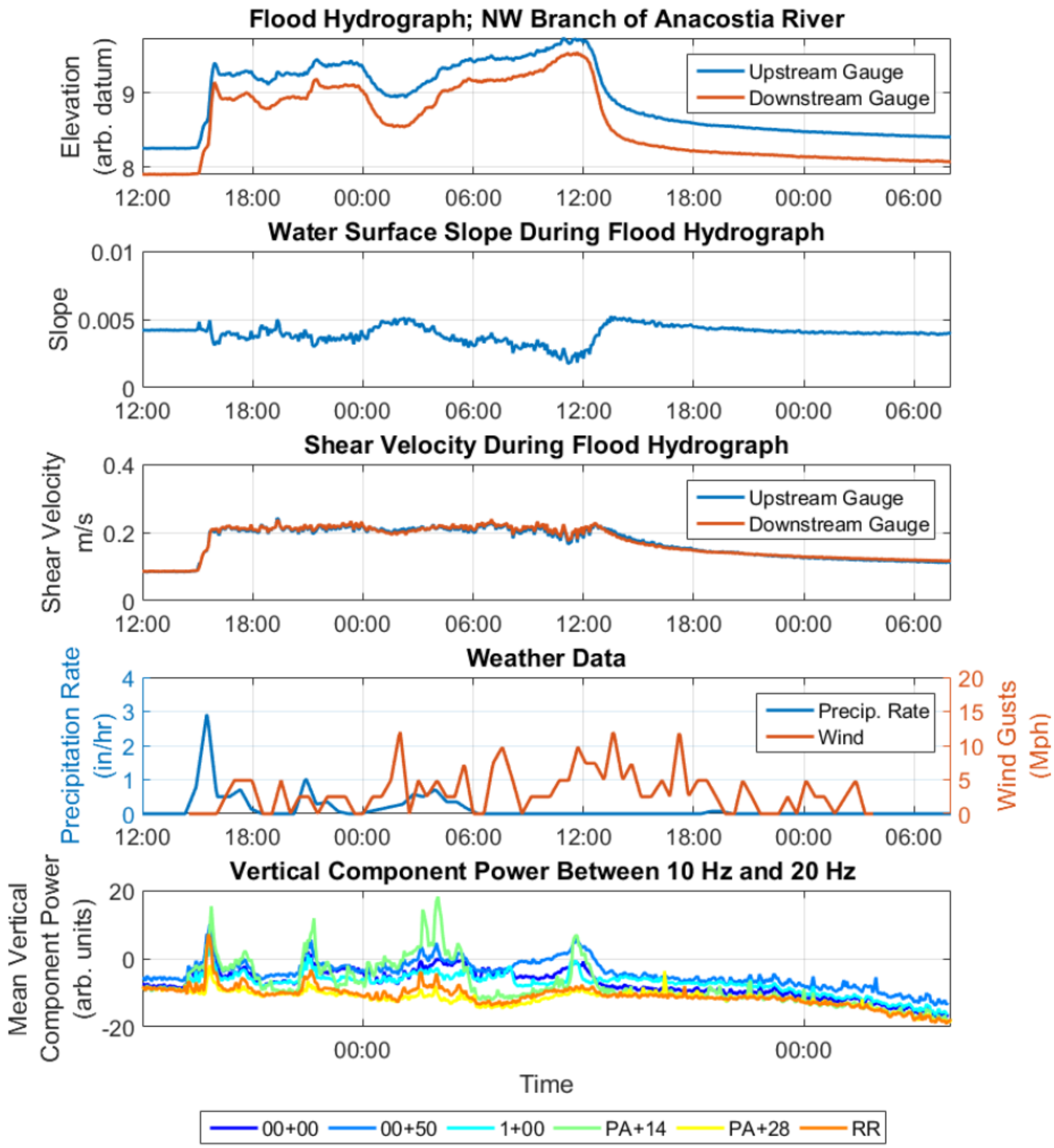

Fig. 3**:** Preliminary data for the first and largest flood event. Lower diagram indicates the seismic power. In the selected frequency range, seismic mean seismic power for the six seismometer responds to both variations in river stage and to weather factors.

An approach to the isolation of river noise during floods

The natural environment is a noisy place during storms; it is particularly noisy during extreme events that we would most like to monitor with non-contact methods such as seismometers. Therefore, we needed to develop methods to exclude noises from other sources and to verify that the river is the source of the noise that we are analyzing. One approach is to identify the direction from which the seismic signal is emanating. To develop these methods, we first examined the seismic signal that was produced by a distinct hydraulic source: the spillway erosion at Oroville dam. The technique applied to Oroville Dam data is Frequency-Dependent Polarization Analysis. This method extracts polarization attributes from a complex-valued eigenvector of the spectral covariance matrix as a function of frequency. The method is particularly suited for identifying the maximum source of ambient energy at a range of frequencies. We evaluated this method for application to fluvial seismology in Goodling, Lekic, and Prestegaard (2018). Our analysis indicated that the location of the greatest seismic energy (excited by the erosional knick-point in the Oroville Dam spillway) could be identified using this technique, and that the location was sufficiently precise to track changes due to progressive erosion of the spillway. We have also been evaluating an alternative method of analysis for characterizing the distribution fluvial-seismic energy excitation. In this alternative analysis, the ground motion at the seismometer in three dimensions is, at each instant, represented as a rotation around an elliptical orbit. At each instant, the position in the orbit (phase) changes, while the dimensions and orientation of the orbit itself change more slowly. The polarization attribute used to determine the direction of the seismic energy is determined from the azimuth of the polarization vector perpendicular to the semimajor and semiminor axis of the particle motion ellipse. Preliminary analysis of seismic data indicates that interfering noises are minimized during the falling limb of flood hydrographs. The instantaneous polarization analysis also indicates that the noise comes from the river during these time periods.

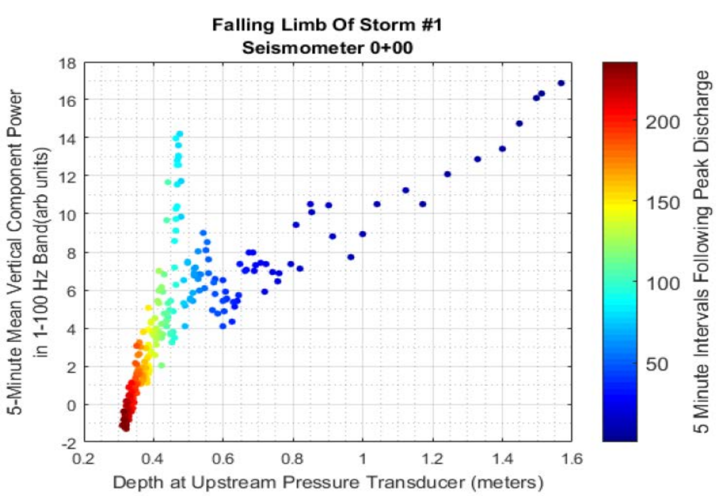

Fig. 4: relationship between flow depth and the 5-minute mean vertical component of Seismic Power during a fall, 2017 hydrograph. The anomaly may be due to wind.

Publications and Presentations:

Goodling, P., Lekic, V., and Prestegaard, K., 2017, "Seismic Analysis of the 2017 Oroville Dam Spillway Erosion Crisis": American Geophysical Union Fall Meeting. New Orleans, Louisiana.

Goodling, P. J., Lekic, V., and Prestegaard, K.: 2018, Seismic signature of turbulence during the 2017 Oroville Dam spillway erosion crisis, Earth Surf. Dynamics. https://doi.org/10.5194/esurf-2017-71

Goodling, P., 2018, "Feel the River Rumble: An introduction to fluvial seismology and its application to the 2017 Oroville Dam spillway erosion crisis" (presentation). USGS MD-DE-DC Water Science Center. Catonsville, MD.

Students Supported or trained:

Undergraduate: Several undergraduate students have assisted in the field with surveying, hydraulic measurements, and the installation of seismometers

M.S.: The project provided primary research funding for Phillip Goodling, a M.S. student in the Geology program co-advised by the PIs. Other M.S. and Ph.D. students studying seismology or geomorphology/hydrology have participated in the research or heard presentations on the project.

Ph.D.: The hydraulic techniques that we developed for this research were used to instrument a tributary junction to obtain time series of shear stress and shear velocity. These data formed the basis for an advanced geomorphology class project. The 7 M.S. and Ph.D. students involved in this project are currently writing up the results of this project for publication.

Assessing nitrate reduction potential in Maryland’s agricultural water resources (Graduate Fellowship)

Basic Information

Title:	Assessing nitrate reduction potential in Maryland’s agricultural water resources (Graduate Fellowship)
Project Number:	2017MD343B
Start Date:	3/1/2017
End Date:	9/30/2017
Funding Source:	104B
Congressional District:	MD 6, 1
Research Category:	Water Quality
Focus Categories:	Nutrients, Non Point Pollution, Agriculture
Descriptors:	None
Principal Investigators:	Eric A Davidson, Kaye Lorraine Brubaker

Publications

There are no publications.

Maryland Water Resources Research Center Summer Graduate Fellowship Progress Report

Jacob Hagedorn
Graduate Student at UMCES Appalachian Laboratory
jhagedorn@umces.edu

Title: Assessing nitrate reduction potential in Maryland's agricultural water resources

Federal Award # to UMCP: #G16AP00061
UMCP subaward to UMCES: # 51388-Z9212103
2017MD343B

Eric Davidson
Professor and Director of UMCES Appalachian Laboratory
edavidson@umces.edu

Background and Objectives

Managing water resources wisely while reducing environment impact is a key component of agricultural sustainability on the Eastern Shore of Maryland. A cornerstone of coastal economies, agricultural practices must find new strategies to effectively reduce nutrient runoff from farmed lands that contribute to contamination of our water resources. Preliminary research suggests that one such water management solution is a water level control device that retains water in drained agricultural fields. The purpose of retaining more water in the fields is to create more anaerobic conditions, which help drive the process of denitrification. Increased denitrification consumes and reduces the nitrate stored in the fields, resulting in an improvement in water quality and reduction in nutrient runoff. While previous studies have shown the nitrate concentrations were reduced in areas with this BMP, there have been limited experiments done to explore and quantify the amount of denitrification occurring in these fields. The reason this is important is because a byproduct of denitrification is nitrous oxide (N_2O) and there is a risk that the water management strategy could increase emissions of this potent greenhouse gas, which would result in an offset of water pollution with air pollution. Therefore, the aim of this research is to demonstrate the efficacy of reducing nutrient runoff compared to risks of increased greenhouse gas emissions for a BMP that has transformative potential in the region. Using a novel research approach that integrates soil gas efflux measurements with isotopic measurements of total denitrification, this study will advance the understanding of agricultural nutrient impacts on Maryland's water resources.

Objective 1: Characterize the nitrogen loading and export from the agricultural fields using mass balance, weirs, stream and soil sampling.

Objective 2: Measure the amount of denitrification on a field-scale level using an isotopic mass balance technique.

Objective 3: Quantify soil gas emissions of N_2O using static soil chambers and Picarro gas

analyzer.
The primary purpose of the summer graduate fellowship funds is to fulfill the objective 2 of this project: to collect and measure the isotopic signatures of nitrate nitrogen and oxygen in groundwater, surface water, and soil.

Summer Activities / Research Methods

Research location and site description
The selected agricultural field site is located on a farm within the Choptank watershed on the coastal plain in Eastern Shore of Maryland (N39.11973, W-75.8069). This is a historically farmed portion of Maryland, with much of the crop product contributing feed to concentrated poultry production. The site was chosen because it is an actively privately farmed area in which cooperation between research and farmer was achieved. About 13 hectares of the site has five ditches that drain the field, each with a drainage control structure (DCS) at the end of the ditch. The ditches roughly split the site into four similarly size fields. The ditches have an average length of 180m.Two fields are serve as a control, with no DWM, and two fields are have actively managed using the DWM design.

Experimental Design
Denitrification has an isotopic influence on nitrate in soils and water. To characterize the overall distribution and effect of denitrification at the site, this design relies on sampling the nitrate content of surface ditch water, piezometer soil water, soil cores, and surface soils. Figure 1 shows a cross section of the relative sample locations within the field.

Nitrate sampling locations
Ditches: Grab samples are taken monthly (some collected by collaborators)
Piezometers: Installed to approximate depth of 1m and sampled monthly (collected by collaborators)
Soil Cores: Soil cores are extracted using a hand auger and subsamples are collected from each 10 cm interval to approximately 100cm depth. Soil cores extracted every two months at each plot per treatment.
Soil Surface: Soils plugs (10 cm) are collected at the surface near the gas flux chambers. Collected monthly.

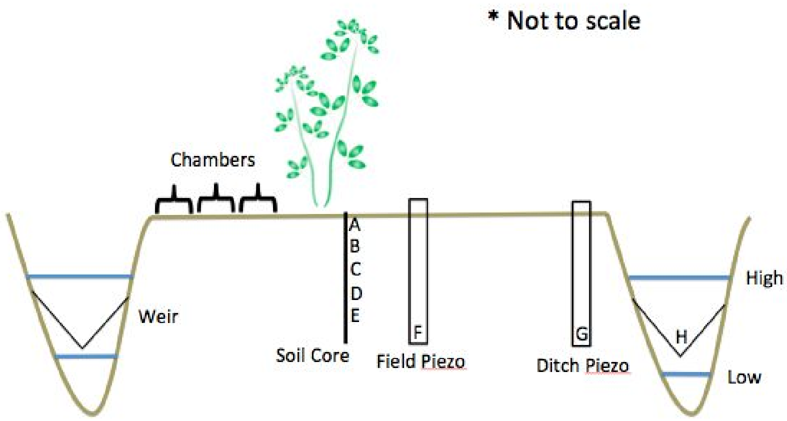

Figure 1. Relative location of ditches, piezometers, and chambers.

To assess the nitrate isotopic signatures and the imprint of denitrification at the field site, Figure 1 depicts specific locations at the site labeled with letters (A-H). The $\delta^{15}N$ and $\delta^{18}O$ isotopic values are plotted for each point specified. It is expected that the denitrification signal is cumulative as water moves from the surface, down the soil profile and into the ditches. Because preliminary data will help shed light on isotopic dynamics at the site, the analysis will develop as preliminary data are analyzed.

The initial expectations are outlined in Figure 2. The upper panel shows that the $\delta^{15}N$ and $\delta^{18}O$ values of nitrate corresponding to each letter in Figure 1. In both the treatment and control sites, this general trend is expected. This is evaluated for each sampling date because each date is associated with a specific set of environmental conditions that impact denitrification by depth. If sampling dates are averaged, those environmental conditions are mixed and therefore the isotopic denitrification signal with depth would be mixed. The purpose of this analysis is to confirm that the imprint of denitrification changes with soil depth and along the transport pathway to the ditch. The slope will be evaluated between each point and also among all points. It is possible that the isotopic values do not change between two points so this analysis will occur at different scales. One scale is evaluating change every 10 cm in the soil profile and the other scale is evaluating the difference between soil surface and ditch water.

The lower panel in Figure 2 shows the expectation that nitrate isotopes in piezometers, ditch water, and bulk soil extracts in control fields have lower $\delta^{15}N$ and $\delta^{18}O$ values compared to the treatment fields. Each sampling date is examined individually and all sampling dates are averaged per time period for this plot. While evidence of denitrification is expected in treatment and control, since the treatment intentionally delays the time it takes for water to move to the ditches, the treatment could show a more significant isotopic signal denitrification earlier in the progression of the sequence from A to H. The amount of nitrate is also expected to be lower earlier in the sequence from A-H. Therefore, for each sampling date, if isotope values were averaged, the treatment $\delta^{15}N$: $\delta^{18}O$ value would be higher than the control. The purpose of this analysis is to directly answer if DWM impacts the isotopic composition of nitrate across all sampling locations.

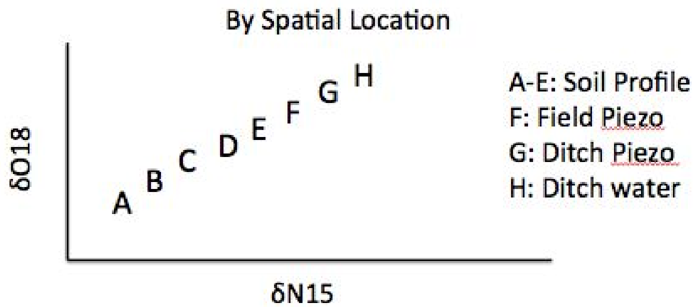

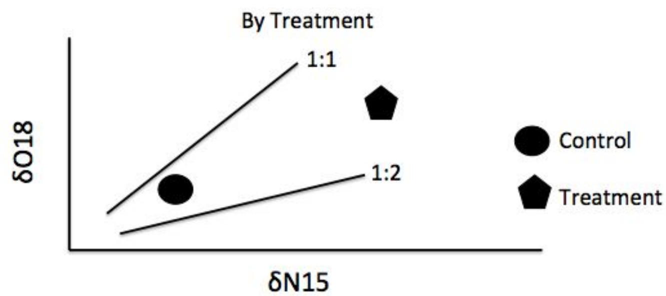

Figure 2. Theoretical expectations of isotopic determination of denitrification analysis. A slope between 1 and 0.5 is indicative of denitrification.

Preliminary Results

Between March 2016 and November 2017 samples were collected at the aforementioned locations and intervals. Utilizing the denitrifier method and the equipment at the Central Appalachians Stable Isotope Facility (CASIF) in Frostburg, MD, soil and water samples were processed and nitrate isotopes were characterized. Because of delays in sample collection and instrument availability, not all samples have been analyzed to date. The results below represent what has been analyzed, with more to come.

Figure 3 shows the distribution of isotopes in a similar format to the theoretical approach represented in the top panel of Figure 2, for one specific date. In the case of Figure 3, points A-J represent soil profile measurements with A at the top of the soil profile and J at the bottom of the soil profile. Points K and L represent piezometer samples. For the following plots, site B is the control plot (no DWM) and site C is the treatment plot (DWM).

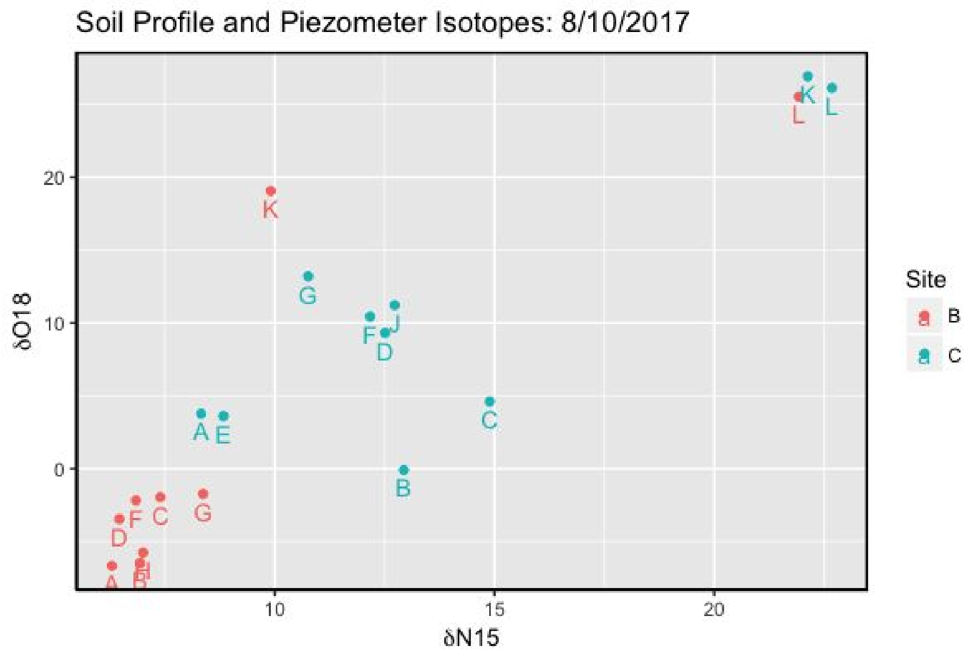

Figure 3. Nitrate isotopes of soil extracts and piezometer samples on 08/10/2017. Points A-J represent the soil profile and points K-L piezometer samples.

For this single snapshot in time, there are a few observations of note. First, there does seem to be a difference in isotope values between site B, the control, and site C, the treatment. It looks like there is more denitrification occurring in the treatment site compared to the control site. Second, both sites indicate dentrification occurring by the time the nitrate reaches the groundwater in the piezometers. Points K and L are distinct from the soil profile points A-J, similar to expectations in the top panel of Figure 2. Third, it looks like site C, the treatment, has more denitrification occurring in the soil profile compared to the control site because of the variation in the isotope measurements A-J.

Piezometer and ditch water samples have yet to be completely analyzed. The goal this summer is to finish analyzing the piezometer and ditchwater samples and to continue collecting and analyzing soil cores.

References

Billy, Claire, et al. "Nitrogen isotopic composition of leached nitrate and soil organic matter as an indicator of denitrification in a sloping drained agricultural plot and adjacent uncultivated riparian buffer strips." Soil Biology and Biochemistry 42.1 (2010): 108-117.

Houlton, Benjamin Z., and Edith Bai. "Imprint of denitrifying bacteria on the global terrestrial biosphere." Proceedings of the National Academy of Sciences 106.51 (2009): 21713-21716.

Kendall, Carol, Emily M. Elliott, and SCOTT D. Wankel. "Tracing anthropogenic inputs of nitrogen to ecosystems." Stable isotopes in ecology and environmental science 2 (2007): 375-449.

Sigman, D. M et al. "A bacterial method for the nitrogen isotopic analysis of nitrate in seawater and freshwater." Analytical chemistry 73.17 (2001): 4145-4153.

Presentations and Publications

1. Hagedorn, J. “Pollution trade-offs for sustainable coastal agricultural management.” Virginia Sea Grant Graduate Symposium. 2018.

2. Hagedorn, J., et al. "Multi-Scale Approach for Measuring N2O and CH4 Emissions in Drainage Water Managed Corn-Soybean System." AGU Fall Meeting Abstracts. 2017.

3. Hagedorn, J. "Food and Stuff." AGU Fall Meeting Abstracts. 2017.

Major ions, strontium isotopes, and geochemical cycling across a forested to urban gradient (Graduate Fellowship)

Basic Information

Title:	Major ions, strontium isotopes, and geochemical cycling across a forested to urban gradient (Graduate Fellowship)
Project Number:	2017MD344B
Start Date:	3/1/2017
End Date:	9/30/2017
Funding Source:	104B
Congressional District:	MD 2
Research Category:	Water Quality
Focus Categories:	Solute Transport, Hydrogeochemistry, Geochemical Processes
Descriptors:	None
Principal Investigators:	Joel Moore, Kaye Lorraine Brubaker

Publications

There are no publications.

Name: Gregory Woodward
Environmental Science and Studies, Towson University

Title: Major ions, strontium isotopes, and geochemical cycling across a forested to urban gradient
MWRRC Grant #: 2017MD344B

Faculty advisor: Dr. Joel Moore: moore@towson.edu

Dear Dr. Brubaker,

Thanks to the grant from you and the Maryland Water Resources Research Center, I had the opportunity and privilege to work on two research projects throughout the summer of 2017. The first was sampling and analysis of water samples from the forested to urban gradient project that was the focus of my proposal. The second was working with samples and data from stormwater management basins, groundwater, and soil cores as part of a project entitled "Strontium Isotopes as a Tracer for Road Salt Transport Through a Shallow Aquifer." Results from this second project will provide important information for understanding road salt and other urban sources contributing to changes in water chemistry across the forested to urban watershed gradient.

Background and Objectives

Every year, millions of pounds of de-icer (road salt), consisting mostly of halite (NaCl) are added to impervious surfaces across the United States. Since the 1970s, road salt use in the US has more than tripled to over 25 million tons per year (Mullaney et al., 2009). As a result, fresh water bodies and drinking water supplies around the eastern US have become increasingly saline with many exceeding the US EPA chronic exposure level of 230 mg/L for chloride (Cl^-) (Cooper et al., 2014; Kaushal et al., 2005; Moore et al., 2017; Mullaney et al., 2009; Novotny et al., 2008; Price and Szymanski, 2014; U.S. EPA, 2017). The salinity increases correlate with growing road salt use and higher impervious surface cover (Dugan et al., 2017; Mullaney et al., 2009).

To date, the impacts of road salt on surface water have been well documented but the impact on soils and aquifers as well as the rates and mechanisms of transport are much less well studied. Differentiating the contributions of road salt to stream chemistry from the contributions due to natural processes can be obscured by natural inputs of Na^+ or Ca^{2+} from carbonate bedrock. Strontium (Sr) isotope ratios ($^{87}Sr/^{86}Sr$) are commonly used for characterizing water-rock interactions, identifying weathering rates, and for tracing the effects of agriculture and urbanization (Böhlke and Horan, 2000; Christian et al., 2011; Shand et al., 2009). In addition,

$^{87}Sr/^{86}Sr$ ratios have been used to identify lithogenic versus atmospheric sources of salinity (Shand et al., 2009). However, there has been minimal research on the use of Sr isotopes to identify road salt influence within soils, surface water, or groundwater. This project seeks to apply the use of Sr isotope ratios to quantitatively describe the impact and transport of road salt on soil, aquifers, and surface water.

Summer Activities and Research Methods

This summer, some time was spent field sampling with some undergraduates for the forested to urban gradient project while most of the time was spent researching, writing, and organizing and analyzing data. The study is being conducted in an urban area near Owings Mills, in Baltimore County, Maryland (fig. 1). The site is a wooded floodplain area approximately 3.5 hectares and is underlain by the Oella schist (Crowley, 1977). Soil at the site is classified as Baile silt loam, a product of schist weathering, which has poor drainage that often results in flooding (USDA, 2017). The Baile soils typically have shallow water tables ranging from 0 to 6 inches below the surface depending on location and time of year (USDA, 2017).

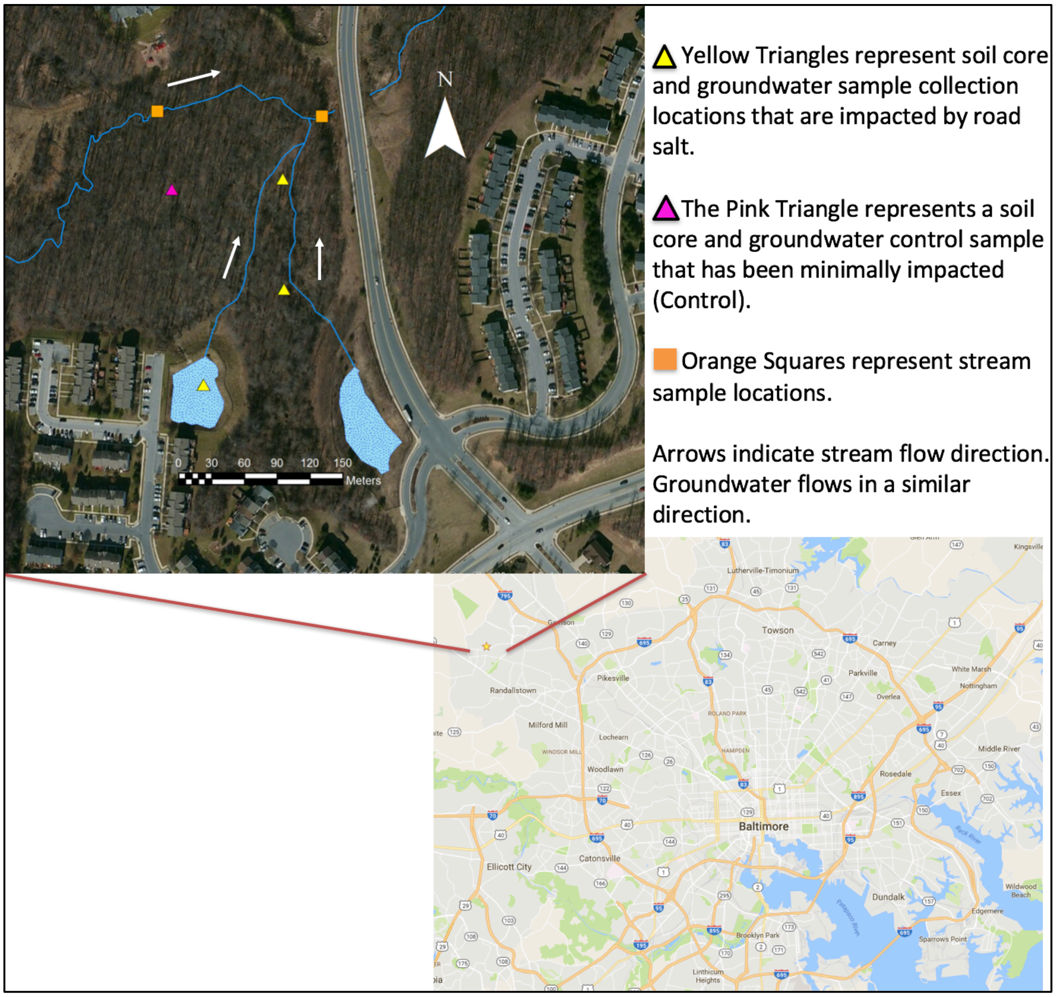

Figure 1: Study Site Location. The Winterset Site is located in Owings Mills, Maryland approximately 6 miles northwest of Baltimore.

Two stormwater management basins (SMBs) designed to capture stormwater and drain within 24-48 hours are present at the site (Moore et al., 2013b; Snodgrass et al., 2017). The SMBs receive water from the roads and parking lots of two condominium neighborhoods in the area. The SMBs release water northward through the floodplain ~200 meters to an unnamed second-order tributary (The stream) of Red Run. Red Run flows to the Gwynns Falls which flows to the Patapsco River and eventually to the Chesapeake Bay. The floodplain at the site acts as a shallow groundwater aquifer with the water table close to the surface throughout most of the year. Groundwater at the site has been shown to flow north-north-east as demonstrated by groundwater modelling of the salt plumes. Therefore, an area along the west side of the floodplain can be used as a control to allow for comparison with water and soil unaffected by the SMBs.

Stream, well, and soil samples were collected from July 2014 through April 2016 and some analyses have already been completed. Rocks used in the SMB fill also have been collected in addition to one road salt sample from the site. To obtain background Sr^{2+} isotope ratios for the site, a sample of the Oella schist will be collected in addition to the fill used in the SMB construction and additional road salt samples collected from the site.

During the sample collection period, the stream was sampled biweekly at both an upstream location before entering the floodplain area and a downstream location after passing through the site (Fig. 1). Several 4-inch diameter monitoring wells were installed in the floodplain of the site as well as in the SMBs. Monitoring wells have been sampled monthly. Soil cores were collected from within the western SMB as well as along the flow transect in the floodplain 100 meters north of the SMB outfall and 200 meters north of the SMB outfall to help provide insight to the relationship between soil and groundwater within the aquifer.

The stream was sampled at an upstream location before entering the floodplain area and a downstream location after passing through the site (Fig. 1). The monitoring wells are pumped until dry approximately 24 hours before sample collection to allow for fresh groundwater recharge. Water samples from both the stream and monitoring wells have been collected for major ion analysis, alkalinity, Sr analysis, pH and specific conductivity. Samples were collected using a peristaltic pump, field filtered (0.45 μm), and collected in LDPE bottles; Sr isotope samples have been collected in I-Chem certified HDPE bottles. Sample bottles were rinsed with sample water before sample collection. Nitrile gloves were worn at all times. pH and conductivity was field measured (non-filtered) using a Thermo Scientific Orion Star A325 portable pH/conductivity meter.

Samples for alkalinity were collected with no headspace and measured within 24 hours. Alkalinity will be calculated using the Gran titration method via a Mettler-Toledo Autotitrator. Major ions will be measured using a Dionex ICS-5000 Ion Chromatograph. Sr concentrations will be measured using an Inductively Coupled Plasma Mass Spectrometer (ICP-MS). Samples will be sent to an external lab for Sr^{2+} isotope analysis via thermal ionization mass spectrometer (TIMS).

To measure and compare exchangeable cations within the soil, the CEC of each sample was analyzed. The CEC was calculated as the sum of the concentrations of all extractable cations, excluding H^+. A 0.1 M $BaCl_2$ extraction process was used (Hendershot and Duquette, 1986). Cations were measured using a Dionex ICS-5000 ion chromatograph. Exchangeable Sr^{2+} will be measured via an ultrapure 1 M NH_4Cl extraction process (Moore et al., 2013a) where 1 g of each soil sample will be reacted with 10 mL of NH_4Cl and then dried. The sample will then be resuspended in 5% HNO_3.

Preliminary Results

A mixing model will be used to calculate the Sr contributions from Oella schist bedrock, carbonate fill rock used in SMB construction, and road salt found within the stream (Capo et al., 1998; Genereux, 1998; Stewart et al., 1998). The mixing model will demonstrate the impact of road salt in the stream that originated from the site. Sr isotope ratios will be compared to the ratio of Ca/Sr and Ba/Sr found within each end member and water sample (Land et al., 2000). Ba and Sr can be found in trace amounts in various minerals with varying weathering rates because Sr substitutes for Ca and Ba substitutes for K. This multiple tracer system of both elements and isotopes allows for clear distinctions between endmembers within the mixing model. Uncertainty analysis for the mixing model will be calculated using a two-component separation formula that allows for calculation of average error and standard deviation of each end member and propagating that uncertainty through to the stream samples (*Genereux*, 1998).

Currently, four water samples (two from the stream and two from groundwater wells) and one local road salt sample have been analyzed for cation and Sr isotope concentrations (Table 1).

Table 1: Preliminary Sr isotope and cation data

	Na (μmol/L)	Ca (μmol/L)	Sr (nmol/L)	$^{87}Sr/^{86}Sr$	Sr/Na
Upstream from Site	964.3	544.9	1625	0.720214	1.685
Downstream from Site	1146	492.2	1342	0.719673	1.171
Floodplain Well	19,430	542.9	881.1	0.709679	0.0453
East SMB Well	96,350	1534	2825	0.710058	0.0293
Local Road Salt	$1.0x10^6$	751.4	3902	0.707176	0.0038

The data show that the stream and groundwater within the floodplain have been impacted by road salt. The upstream sample location was found to have 964.3 μmol/L of Na^+ while downstream contained 1146 μmol/L of Na^+ indicating the influence of road salt from the SMBs. Na^+ in the floodplain well was found to have a concentration of 19,430 μmol/L while Na^+ concentration inside the SMB reached 96,350 μmol/L. Analysis of $^{87}Sr/^{86}Sr$ data compared with Sr/Na concentration ratios reveals that groundwater at the site shows a similar chemical signature to road salt collected at the site (Fig. 2). In addition, stream water appears to have been affected by road salt from the site, the upstream location shows a higher $^{87}Sr/^{86}Sr$ and Sr/Na value than the downstream collection point. Data collected during the summer from the forest to urban project (fig. 3) shows similar trends to data collected from 2014-2016 when comparing specific conductance to impervious surface coverage (fig. 4) (Moore et al., 2017).

The next steps of the project are to begin Sr extractions for the soil samples and organizing/selecting water samples to be sent to the external lab for sample analysis. This knowledge can be applied to other urban areas as well. The forested to urban project has also begun to collect samples for Sr isotope analysis. Future work will likely include more detailed information regarding solute sources, made possible by Sr isotope analysis.

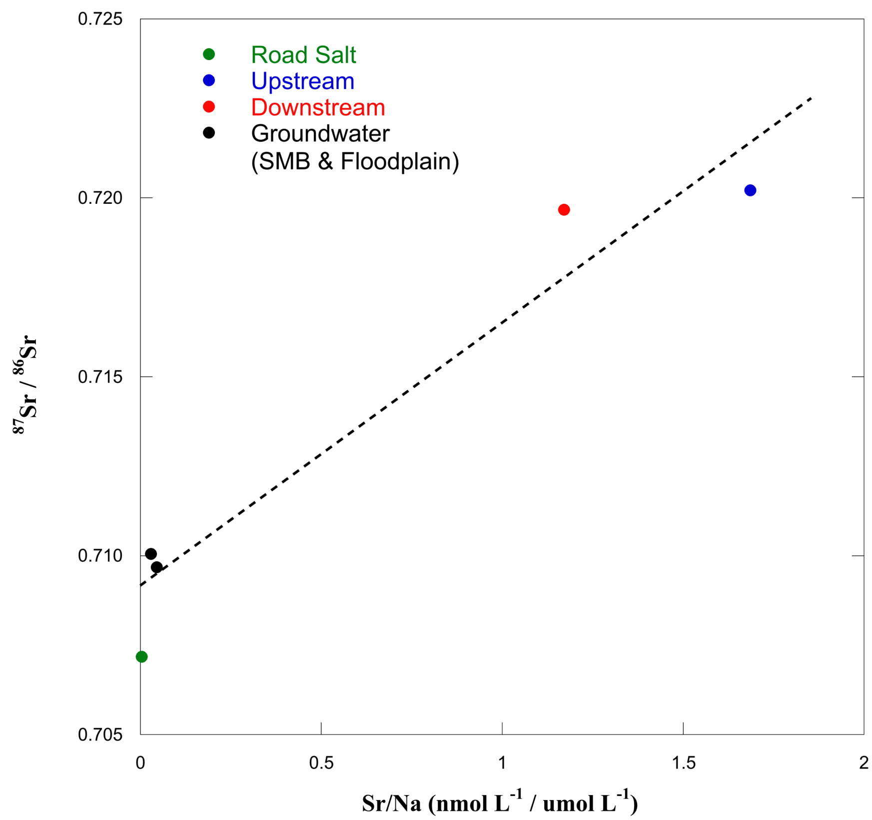

Figure 2: $^{87}Sr/^{86}Sr$ compared with Sr/Na ratios. Surface and groundwater at the site appears to have been affected by road salt use. Road salt from the site has a low $^{87}Sr/^{86}Sr$ value when compared with that of the upstream sample location. The groundwater locations more closely resemble the chemistry of the road salt, while the downstream location also shows impact. The dashed line represents a trend line with an equation of $y=0.0075x + 0.709$ and has an R^2 value of 0.93419.

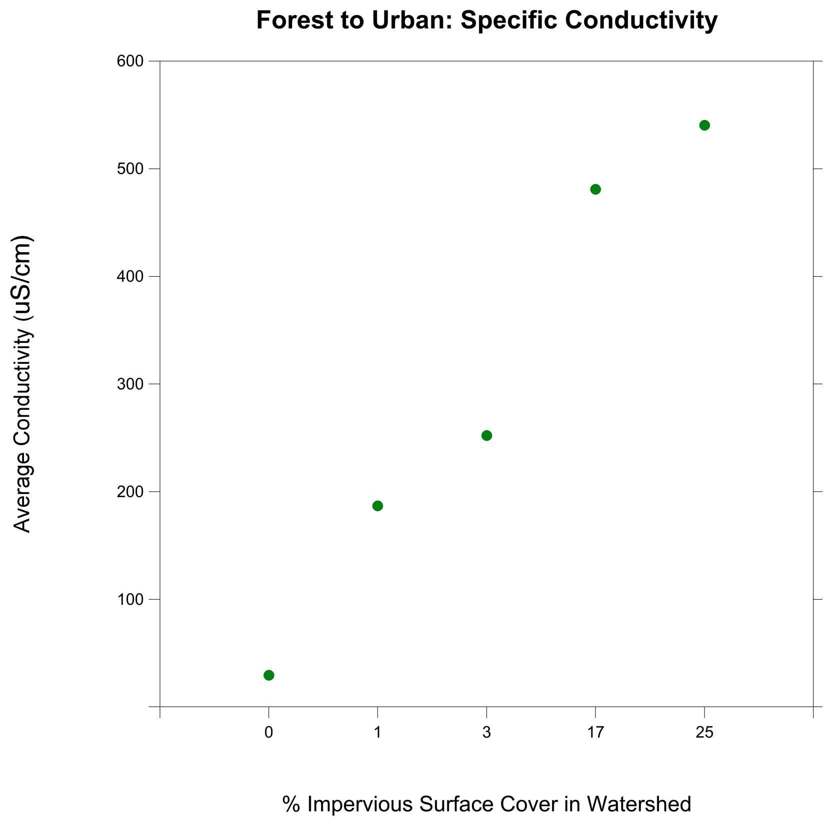

Figure 3: Average specific conductance from the month of June 2017 compared to percent of impervious surface coverage in the watershed. Specific conductance increases with increasing impervious surface coverage.

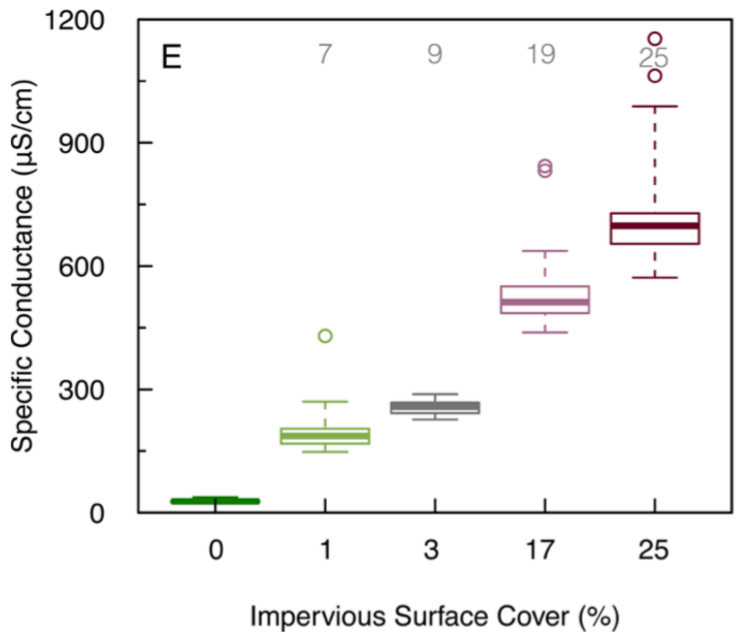

Figure 4: Specific conductance collected between 2014-2016 compared with percent impervious surface coverage. The thick bar in the center of the box plots represents the median concentration in each watershed. Plot whiskers represent four times the interquartile range. (Moore et al., 2017)

References

Böhlke, J.K.; M., Horan, 2000, Strontium isotope geochemistry of groundwaters and streams affected by agriculture, Locust Grove, MD, Applied Geochemistry, 15, 599–609. doi:10.1016/S0883-2927(99)00075-X

Capo, R.C.; B.W., Stewart; O.A., Chadwick, 1998, Strontium isotopes as tracers of ecosystem processes: theory and methods, Geoderma, 197–225.

Christian, L.N.; J.L., Banner; L.E., Mack, 2011, Sr isotopes as tracers of anthropogenic influences on stream water in the Austin, Texas, area, Chemical Geology, 282, 84–97. doi:10.1016/j.chemgeo.2011.01.011

Cooper, C. a.; P.M., Mayer; B.R., Faulkner, 2014, Effects of road salts on groundwater and surface water dynamics of sodium and chloride in an urban restored stream, Biogeochemistry, 1–18. doi:10.1007/s10533-014-9968-z

Crowley, W.P., 1977, Geologic Map of the Reisterstown Quadrangle, Maryland.

Dugan, H.A.; S.L., Bartlett; S.M., Burke; J.P., Doubek; F.E., Krivak-Tetley; N.K., Skaff; J.C., Summers; K.J., Farrell; I.M., McCullough; A.M., Morales-Williams; D.C., Roberts; Z., Ouyang; F., Scordo; P.C., Hanson; K.C., Weathers, 2017, Salting our freshwater lakes, Proceedings of the National Academy of Sciences, 114, 4453–4458. doi:10.1073/pnas.1620211114

Genereux, D., 1998, Quantifying uncertainty in tracer-based hydrograph separations, Water Resources Research, 34, 915–919. doi:10.1029/98WR00010

Hendershot, W.H.; M., Duquette, 1986, A Simple Barium Chloride Method for Determining Cation Exchange Capacity and Exchangeable Cations, Soil Science Society of America Journal, 50, 605–608. doi:10.2136/sssaj1986.03615995005000030013x

Kaushal, S.S., P.M., Groffman; G.E., Likens; K.T., Belt; W.P., Stack; V.R., Kelly; L.E., Band; G.T., Fisher, 2005, Increased salinization of fresh water in the northeastern United States. Proceedings of the National Academy of Science, U. S. A., 102, 13517–13520. doi:10.1073/pnas.0506414102

Land, M.; J., Ingri, P.S., Andersson; B., Öhlander, 2000, Ba/Sr, Ca/Sr and 87Sr/86Sr ratios in soil water and groundwater: Implications for relative contributions to stream water discharge, Applied Geochemistry, 15, 311–325. doi:10.1016/S0883-2927(99)00054-2

Moore, J.; D.L., Bird; S.K., Dobbis; G., Woodward, 2017, Nonpoint Source Contributions Drive Elevated Major Ion and Dissolved Inorganic Carbon Concentrations in Urban Watersheds, Environmental Science and Technology Letters, 4. doi:10.1021/acs.estlett.7b00096

Moore, J.; A.D., Jacobson; C., Holmden; D., Craw, 2013a, Tracking the relationship between mountain uplift, Silicate weathering, And long-term CO2 consumption with Ca isotopes: Southern Alps, New Zealand, Chemical Geology, 341, 110–127. doi:10.1016/j.chemgeo.2013.01.005

Moore, J., Lev, S.M., Casey, R.E., 2013b. Modeling the effects of road salt on soil, aquifer, and stream chemistry.

Mullaney, J.R.; D.L., Lorenz; A.D., Arntson; 2009, Chloride in Groundwater and Surface Water in Areas Underlain by the Glacial Aquifer System, Northern United States Scientific Investigations, Report 2009 – 5086.

Novotny, E. V; D., Murphy; H.G., Stefan, 2008, Increase of urban lake salinity by road deicing salt, Science of the Total Environment, 406, 131–144. doi:http://dx.doi.org/10.1016/j.scitotenv.2008.07.037

Price, J.R.; D.W., Szymanski, 2014, The Effects of Road Salt on Stream Water Chemistry in Two Small Forested Watersheds, Catoctin Mountain, Maryland, USA, Aquatic Geochemistry, 20, 243–265. doi:10.1007/s10498-013-9193-8

Shand, P.; D.P.F., Darbyshire; A.J., Love; W.M., Edmunds, 2009, Sr isotopes in natural waters: Applications to source characterisation and water-rock interaction in contrasting landscapes, Applied Geochemistry, 24, 574–586. doi:10.1016/j.apgeochem.2008.12.011

Snodgrass, J.W.; J., Moore; S.M., Lev; R.E., Casey; D.R., Ownby; R.F., Flora; G., Izzo, 2017, Influence of Modern Stormwater Management Practices on Transport of Road Salt to Surface Waters, Environmental Science and Technology, 51, 4165–4172. doi:10.1021/acs.est.6b03107

Stewart, B.W.; R.C., Capo; O.A., Chadwick, 1998, Quantitative strontium isotope models for weathering, pedogenesis and biogeochemical cycling, Geoderma, 82, 173–195.

United Statets Department of Agriculture – Natural Resources Conservation Service, n.d., Web Soil Survey, National Cooperative Soil Survey [WWW Document]. URL https://websoilsurvey.sc.egov.usda.gov/App/WebSoilSurvey.aspx (accessed 7.20.17).

United States Environmental Protection Agency (USEPA), 2017, National recommended water Quality criteria - Aquatic life criteria table [WWW Document], URL https://www.epa.gov/wqc/national-recommended-water-quality-criteria-aquatic-life-criteria-table (accessed 7.31.17).

Seismo-Acoustic Observation of Cavitation and Erosive Potential in a Bedrock River (Graduate Fellowship)

Basic Information

Title:	Seismo-Acoustic Observation of Cavitation and Erosive Potential in a Bedrock River (Graduate Fellowship)
Project Number:	2017MD345B
Start Date:	3/1/2017
End Date:	9/30/2017
Funding Source:	104B
Congressional District:	MD 5
Research Category:	Climate and Hydrologic Processes
Focus Categories:	Geomorphological Processes, Sediments, Surface Water
Descriptors:	None
Principal Investigators:	Karen Prestegaard, Kaye Lorraine Brubaker

Publications

There are no publications.

Introductory Information

Student Name: Phillip Goodling

Department and University: University of Maryland College Park, Department of Geology

Title of Summer Fellowship Project: "Seismo-Acoustic Observation of Cavitation and Erosive Potential in a Bedrock River"

Number of MWRRC Grant: 2017MD345B

Faculty Advisor Name and Email Address: Dr. Karen Prestegaard, kpresto@umd.edu

Background and Objectives

The research focus this summer was to develop new geophysical tools for evaluating the erosive potential of floods in bedrock rivers. This summer was devoted to developing the foundational work for the following two objectives:

Objective 1: Develop acoustic detection of cavitation in a bedrock stream

Cavitation is the phenomenon where a local drop in pressure below the vapor pressure of the fluid causes a vapor bubble to form. When the bubble moves into an area of higher pressure, it collapses violently, which may cause erosional damage. This process is acoustically observed in engineered structures where high flow velocities in pipe constrictions, propellers, or dam spillways generate high frequency noise. The first theoretical evaluation of cavitation as a force of bedrock erosion was by Barnes (1956) who hypothesized that common bedrock channel erosional features such as flutes and potholes are formed by sediment abrasion and cavitation acting in concert. In-situ acoustic detection represents a possible way to evaluate the potential for bedrock erosion by cavitation.

Objective 2: Develop seismic observation of erosive power and flow resistance in a bedrock stream.

The relationship between river discharge (Q), and average velocity at a river cross section (V), depends on the channel geometry, energy slope, fluid viscosity, and flow resistance, which encompasses dissipative energy losses from turbulence within the flow (Dingman, 1984). For half a century, river scientists have struggled to quantify flow resistance in natural channels, particularly where channels have a complex geometry as in bedrock channels (Powell, 2014). River turbulence and bedload impacts both generate small ground vibrations (microseisms), which radiate to the river banks. Monitoring techniques based on near-channel microseism observations have the potential to replace labor-intensive, hazardous, or unreliable in-stream monitoring methods with a continuous reach-averaged proxy for flow resistance. By applying new computational techniques, the approximate channel sources of resistance could be resolved with microseism observations.

Research Methods and Results

Objective 1: Cavitation Detection

To develop an in-situ technique of acoustic cavitation detection, laboratory recordings of cavitation were performed using an Aquarian Scientific AS-1 hydrophone. Cavitation was created in a quiet laboratory using both a pinched-hose technique and by creating shaped glass venturi tubes. Matlab was used to process the acoustic signals to evaluate the spectral characteristics of cavitation-generated noise. To determine if a 30-foot hydraulic flume at the University of Maryland could be used in a manipulative controlled experiment of cavitation in flows of known velocity, a series of recordings were conducted at varying discharge. A frequency analysis of the background noise of the hydraulic flume indicates that the peak frequency of the noise is sensitive to the discharge (Fig.1). The background frequency peaks occur in the expected range of cavitation (15-40 kHz), therefore, it appears that the pump within the flume creates cavitation, making the flume a poor choice for cavitation experiments.

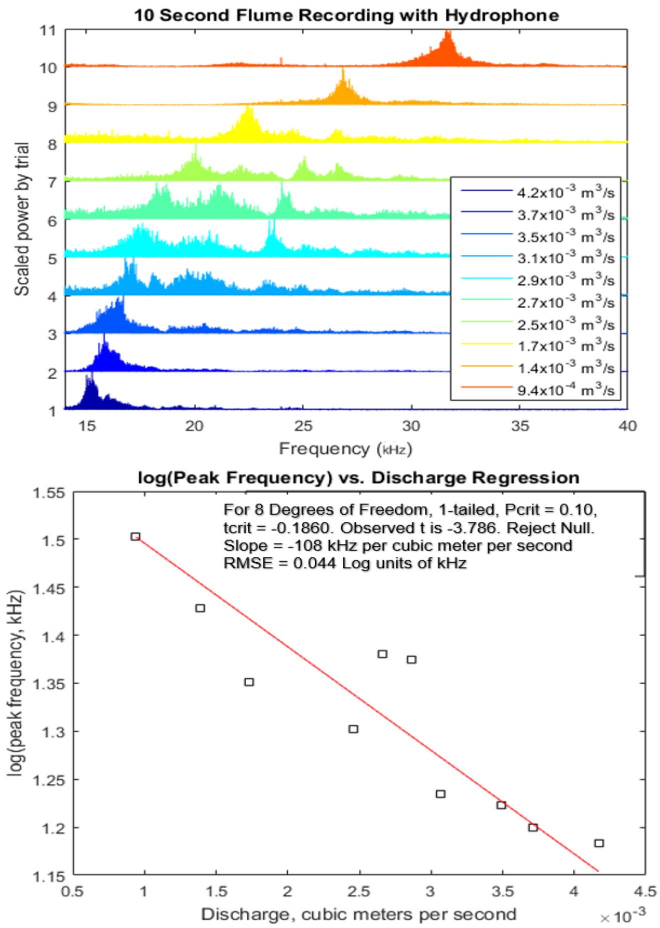

Figure 1- *Top:* The scaled power-frequency distribution of ten recordings of the operating flume at varying discharges. *Bottom:* The frequency peak moves to higher frequencies at lower discharge as the pump becomes more constricted.

To evaluate whether cavitation could occur at the bedrock field site, I compiled hydrologic and geomorphic data for a study reach along a knickzone on the Northwest Branch of the Anacostia river. Data were obtained from USGS gauge data from the Northwest Branch of the Anacostia River, a 1-meter resolution digital elevation model (DEM), and field data collected by McCleaf (2006) during an 8-year flood at the field site. I evaluated hydraulic conditions at the knickzone using the Bernoulli-based analysis of Whipple et al., (2000). From this analysis, I identified locations where cavitation was likely achieved during the 8-year flood monitored by McCleaf (2008).

Objective 2: In-stream seismic observations

In summer 2017, , a seismic observation a 120-meter study reach was set up on the Northwest Branch of the Anacostia River, following official permission from the Maryland National Capital Park and Planning Commission. River cross sections were surveyed at 10 channel locations using a survey level, and three pressure transducers and a barometric sensor were installed. An array of six continuously recording Fairfield Nodal three-component seismometers was installed along the banks of the Anacostia River in the configuration shown in Figure 2. These seismometers record continuously for approximately 30 days. Continuous stage and seismic data were obtained from July 27th through mid-September. This record contains11 storm hydrographs, including one event that raised the river stage at the study reach by ~1.5 meters. Stage data from the study reach and USGS discharge data are used to construct local rating curves. Discharge and local gauge data are used to generate continuous records of mean cross-sectional velocity, energy slope, local flow resistance, and reach flow resistance. .

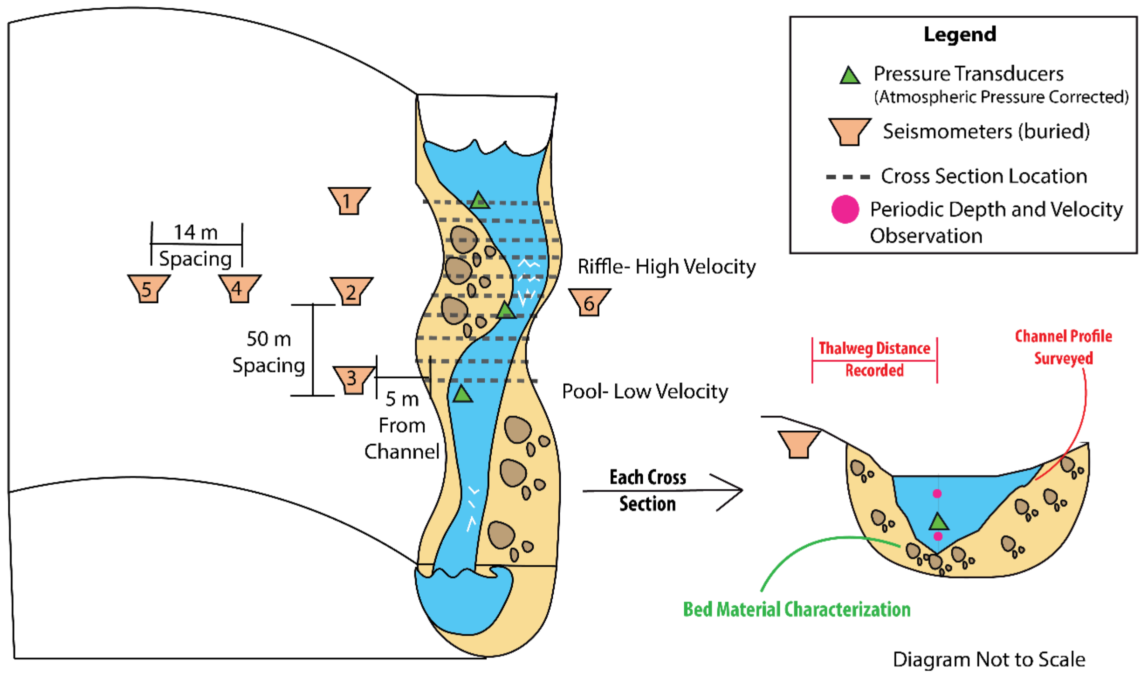

Figure 2- The study reach initiated on the Northwest Branch of the Anacostia river this summer consisted of six seismometers, three pressure transducers, and a barometric pressure sensor.

While seismic data and hydraulic data were being collected, I developed a set of analytical codes in Matlab that will be used to process the seismic data on a flood-by-flood basis. These analyses include implementation of frequency-dependent polarization analysis (Park et al., 1987) and instantaneous polarization analysis (Morozov and Smithson, 1996). These sets of codes will be used to identify the primary source azimuth of the seismic energy recorded at each seismometer. This can be used to track the location of turbulent energy expenditure during the course of a flood event. These codes were tested using seismic data recorded next to the outflow of the Oroville Dam in California; the location of the outflow was resolved using these codes, particularly at high outflows (Goodling et al., 2017a, Goodling et al., 2017b). Applying these methods, which are typically used to characterize ambient seismic noise (e.g. Workman et al., 2017) to the Northwest Branch seismic observations is a novel application of these techniques. Preliminary results of the data analysis show that the seismic observations are quite sensitive to the discharge in the 30 to 55 Hz frequency range, which is similar to that observed by Roth et al. (2017). For the present configuration, the results are most sensitive to changes in amplitude when the river stage is 0.35 m above baseflow. Hysteresis in the stage vs. seismic power relationship at some frequencies is interpreted as indicating bedload transport in the reach, as observed by other researchers (e.g. Roth et al (2017). Polarization results indicate that stations adjacent to the river are sensitive to changes in the seismic character with changes in river discharge.

Lessons Learned and Next Steps

Objective 1:

Fourier analysis of the signal from benchtop recording indicates the frequency peak of cavitation produced this way is typically 5-10 kHz and is readily identifiable in benchtop studies. However, the 30-foot hydraulic flume is not suitable for acoustic measurements of cavitation, as the internal mechanism of the pump produces cavitation noise. Further steps include river observation of the storm flow with the hydrophone.

Objective 2:

Seismic and and hydraulic data have been successfully monitored at the first study site for several stormflow hydrographs. Continual observation of the selected river reach for several more months will allow a range of flood responses to be evaluated. Building on the lessons learned from this first deployment, we plan to create a second array of seismometers on the Paint Branch in an adjacent watershed. This will allow us to investigate the influence of grain size on the seismic signal, as predicted by theoretical models (Gimbert et al. (2014).

The codes built while analyzing data from the Oroville Dam spillway are now directly applicable to river data collected over the coming months. A description of the codes and preliminary analysis was presented at a European Geophysical Union meeting (Goodling et al., 2017). A manuscript of these analyses is being prepared for submission to the Journal of Earth Surface Dynamics. An abstract was submitted to the American Geophysical Union for the Fall Meeting (Goodling et al., 2017b) that will feature seismic data from both Oroville Dam and the Northwest branch of the Anacostia River. Maryland Water Resources Research Center grant funding was acknowledged will be acknowledged in both journal article and conference presentations.

References

Barnes, H. L., 1956, Cavitation as Geological Agent: American Journal of Science, v. 254, p. 493-505.

Dingman, S.L., 1984, Fluvial Hydrology. W.H. Freeman and Co., NY

Gimbert, F., V. C. Tsai, and M. P. Lamb, 2014, A physical model for seismic noise generation by turbulent flow in rivers: Journal of Geophysical Research-Earth Surface, v. 119, p. 2209-2238.

Goodling, P.J., V. Lekic, and K.P. Prestegaard, 2017a, Interpreting Microseismic Energy Produced By The 2017 Oroville Dam Crisis “in” From Process to Signal- Advancing Environmental Seismology Abstracts, Ohlstadt, Germany, 6-9 June.

Goodling, P.J., V. Lekic, and K.P. Prestegaard, 2017b, Abstract #246593 - Seismic Analysis of the 2017 Oroville Dam Spillway Erosion Crisis “in” 2017 AGU Fall Meeting Abstracts, New Orleans, LA, 11-15 Dec.

McCleaf, A.A., 2006, Hydraulics Affecting Bedrock Erosion at a Stream Knickpoint. Senior Thesis, University of Maryland College Park Department of Geology. Accessed at: https://www.geol.umd.edu/undergraduate/paper/mccleaf.pdf

Morozov, I. B., and S. B. Smithson, 1996, Instantaneous polarization attributes and directional filtering: Geophysics, v. 61, p. 872-881.

Park, J., F. L. Vernon, and C. R. Lindberg, 1987, Frequency-Dependent Polarization Analysis Of High-Frequency Seismograms: Journal of Geophysical Research-Solid Earth and Planets, v. 92, p. 12664-12674.

Powell, D. M., 2014, Flow resistance in gravel-bed rivers: Progress in research: Earth-Science Reviews, v. 136, p. 301-338.

Roth, D. L., N. J. Finnegan, E. E. Brodsky, D. Rickenmann, J. M. Turowski, A. Badoux, and F. Gimbert, 2017, Bed load transport and boundary roughness changes as competing causes of hysteresis in the relationship between river discharge and seismic amplitude recorded near a steep mountain stream: Journal of Geophysical Research-Earth Surface, v. 122, p. 1182-1200.

Whipple, K. X., G. S. Hancock, and R. S. Anderson, 2000, River incision into bedrock: Mechanics and relative efficacy of plucking, abrasion, and cavitation: Geological Society of America Bulletin, v. 112, p. 490-503.

Information Transfer Program Introduction

None.

USGS Summer Intern Program

None.

Student Support					
Category	**Section 104 Base Grant**	**Section 104 NCGP Award**	**NIWR-USGS Internship**	**Supplemental Awards**	**Total**
Undergraduate	1	0	0	0	1
Masters	3	0	0	0	3
Ph.D.	3	0	0	0	3
Post-Doc.	0	0	0	1	1
Total	7	0	0	1	8

Notable Awards and Achievements

Publications from Prior Years

1. 2015MD329B ("Retrospective Analysis of Nutrient and Sediment Loadings and Trends in the Chesapeake Bay Watershed (Graduate Fellowship)") - Articles in Refereed Scientific Journals - Zhang, Qian, Ciaran J. Harman, James W. Kirchner, 2018, Evaluation of statistical methods for quantifying fractal scaling in water-quality time series with irregular sampling, Hydrology and Earth System Sciences, 22(2), DOI 10.5194/hess-22-1175-2018
2. 2012MD299S ("The Effectiveness of a Computer-Assisted Decision Support System Using Realistic Interactive Visualization as a Learning Tool in Flood Risk Management") - Articles in Refereed Scientific Journals - Olsen, V. B. Kuser, B. Momen, S.M. Langsdale, G.E. Galloway, E. Link, K.L. Brubaker, M. Ruth, R.L. Hill, 2018, An approach for improving flood risk communication using realistic interactive visualisation, Journal of Flood Risk Management, 11, S783-S793, DOI 10.1111/jfr3.12257.
3. 2015MD332B ("Storm Water Runoff and Water Quality Modeling in Urban Maryland (Graduate Fellowship)") - Articles in Refereed Scientific Journals - Wang, Jing, Barton A. Forman, Allen P. Davis, 2018, Probabilistic Stormwater Runoff and Water Quality Modeling of a Highway in Suburban Maryland, Journal of Hydrologic Engineering, 23(2), DOI DI 10.1061/(ASCE)HE.1943-5584.0001600
4. 2015MD330B ("Chironomus riparius: A Tool for Studying Ecological Effects of “Inert” Safeners (Graduate Fellowship)") - Articles in Refereed Scientific Journals - Bolyard, Kasey, Susan E. Gresens, Allison N. Ricko, John D. Sivey, and Christopher J. Salice, 2017, ASSESSING THE TOXICITY OF THE "INERT" SAFENER BENOXACOR TOWARD CHIRONOMUS RIPARIUS: EFFECTS OF AGROCHEMICAL MIXTURES, Environmental Toxicology and Chemistry, 36(10), pp. 3660-2670, DOI 10.1002/etc.3814
5. 2010MD229B ("Occupational and Community Exposure to Antimicrobial-Resistant Bacteria and Antimicrobials Present in Reclaimed Wastewater ") - Articles in Refereed Scientific Journals - Goldstein, Rachel Rosenberg, Lara Kleinfelter, Xin He, Shirley A. Micallefr, Ashish George, Shawn G. Gibbs, and Amy R. Sapkota, 2017, Science of the Total Environment, 595, pp. 35-40, DOI 10.1016/j.scitotenv.2017.03.174
6. 2014MD315B ("Validation of non-lethal laparoscopic technique for detection of intersex in regional black bass populations") - Articles in Refereed Scientific Journals - Alexander H. MacLeod, Vicki S. Blazer, Mark A. Matsche, and Lance T. Yonkos, 2017, NONLETHAL LAPAROSCOPIC DETECTION OF INTERSEX (TESTICULAR OOCYTES) IN LARGEMOUTH BASS (MICROPTERUS SALMOIDES) AND SMALLMOUTH BASS (MICROPTERUS DOLOMIEU), Environmental Toxicology and Chemistry, 36(7), pp. 1924-1933, DOI 10.1002/etc.3716